Received: 3 October 2022 | Revised: 14 December 2022 | Accepted: 30 December 2022

DOI: 10.1111/bph.16033

RESEARCH ARTICLE

The P2X7 receptor contributes to seizures and inflammation-driven long-lasting brain hyperexcitability following hypoxia in neonatal mice

Jonathon Smith[1,2] | Aida Menéndez Méndez[1] | Mariana Alves[1] | Alberto Parras[3] | Giorgia Conte[1] | Anindya Bhattacharya[4] | Marc Ceusters[5,6] | Annette Nicke[7] | David C. Henshall[1,2] | Eva M. Jimenez-Mateos[8] | Tobias Engel[1,2]

[1]Department of Physiology and Medical Physics, RCSI University of Medicine and Health Sciences, Dublin, Ireland

[2]FutureNeuro, SFI Research Centre for Chronic and Rare Neurological Diseases, RCSI University of Medicine and Health Sciences, Dublin, Ireland

[3]Department of Biomedical Sciences, Faculty of Biology and Medicine, University of Lausanne, Lausanne, Switzerland

[4]Neuroimmunology Discover, Neuroscience, Janssen R&D, San Diego, California, USA

[5]Neuroscience Therapeutic Area, Janssen Research and Development, Janssen Pharmaceutica NV, Beerse, Belgium

[6]The Marc Ceusters Company BV, Diest, Belgium

[7]Walther Straub Institute of Pharmacology and Toxicology, Ludwig Maximilian University of Munich, Munich, Germany

[8]Discipline of Physiology, School of Medicine, Trinity Biomedical Sciences Institute, Trinity College Dublin, The University of Dublin, Dublin, Ireland

Correspondence
Tobias Engel, Department of Physiology and Medical Physics, RCSI University of Medicine and Health Sciences, Dublin D02 YN77, Ireland.
Email: tengel@rcsi.ie

Eva M. Jimenez-Mateos, Discipline of Physiology, School of Medicine, Trinity Biomedical Sciences Institute, Trinity College Dublin, The University of Dublin, Dublin, Ireland.
Email: jimeneze@tcd.ie

Funding information
Deutsche Forschungsgemeinschaft, Grant/Award Numbers: 335447717 - SFB 1328, 335447717—SFB 1328; Science Foundation Ireland, Grant/Award Numbers: 16/RC/3948, 17/CDA/4708; H2020 Marie Skłodowska-Curie Actions, Grant/Award Numbers: 766124, 884956; Irish Research Council for Science, Engineering and Technology, Grant/Award Number: GOIPD/2020/865

Background and Purpose: Neonatal seizures represent a clinical emergency. However, current anti-seizure medications fail to resolve seizures in ~50% of infants. The P2X7 receptor (P2X7R) is an important driver of inflammation, and evidence suggests that P2X7R contributes to seizures and epilepsy in adults. However, no genetic proof has yet been provided to determine what contribution P2X7R makes to neonatal seizures, its effects on inflammatory signalling during neonatal seizures, and the therapeutic potential of P2X7R-based treatments on long-lasting brain excitability.

Experimental Approach: Neonatal seizures were induced by global hypoxia in 7-day-old mouse pups (P7). The role of P2X7Rs during seizures was analysed in P2X7R-overexpressing and knockout mice. Treatment of wild-type mice after hypoxia with the P2X7R antagonist JNJ-47965567 was used to determine the effects of the P2X7R on long-lasting brain hyperexcitability. Cell type-specific P2X7R expression was analysed in P2X7R-EGFP reporter mice. RNA sequencing was used to monitor P2X7R-dependent hippocampal downstream signalling.

Key Results: P2X7R deletion reduced seizure severity, whereas P2X7R overexpression exacerbated seizure severity and reduced responsiveness to anti-seizure

Abbreviations: ASM, anti-seizure medication; FjB, Fluoro-Jade B; HIE, hypoxic–ischaemic encephalopathy; NE, neonatal encephalopathy; P7, seven days post-natal; P2X7R-OE, P2X7R overexpression; TH, therapeutic hypothermia.

Jonathon Smith, Aida Menéndez Méndez, Eva M. Jimenez-Mateos and Tobias Engel contributed equally to this work.

medication. P2X7R deficiency led to an anti-inflammatory phenotype in microglia, and treatment of mice with a P2X7R antagonist reduced long-lasting brain hyperexcitability. RNA sequencing identified several pathways altered in P2X7R knockout mice after neonatal hypoxia, including a down-regulation of genes implicated in inflammation and glutamatergic signalling.

Conclusion and Implications: Treatments based on targeting the P2X7R may represent a novel therapeutic strategy for neonatal seizures with P2X7Rs contributing to the generation of neonatal seizures, driving inflammatory processes and long-term hyperexcitability states.

KEYWORDS

inflammation, neonatal seizures, P2X7 receptor, purinergic signalling

1 | INTRODUCTION

Neonatal seizures, one of the most common neurological emergencies during the neonatal period, affect up to 5/1000 full-term infants and represent a significant risk factor for mortality (Glass et al., 2016; Pressler et al., 2021). The most common cause is a loss of oxygen and glucose supply to the brain (~40% of cases), known as hypoxic–ischaemic encephalopathy (HIE). Other aetiologies include placental pathologies, brain malformations, infections, genetic syndromes and metabolic problems (Pressler et al., 2021). The current standard of care with HIE patients is to initiate therapeutic hypothermia (TH) (Jensen, 2009). TH has, however, limited effectiveness to reduce seizures in more severe HIE cases and may have limited impact on later-life co-morbidities (Hellstrom-Westas et al., 2015). First-line pharmacological treatment for neonatal seizures is with **phenobarbital**. If unsuccessful, patients will commonly be prescribed with additional anti-seizure medications (ASMs) including **phenytoin**, **levetiracetam** or **midazolam** (Hellstrom-Westas et al., 2015). Current ASMs have, however, a poor response rate (e.g., ~60% for phenobarbital) (Wagner et al., 2021), also may cause adverse effects on neurodevelopment (Quinlan et al., 2018), and have limited efficacy at preventing the later development of epilepsy (Ramantani et al., 2019).

Elevated neuroinflammation is well established following neonatal seizures (Leavy & Jimenez Mateos, 2020). Cellular components such as microglia perform critical homeostatic functions during early brain development, but when inflammation becomes excessive or prolonged, this can drive enduring states of hyperexcitability (Vezzani et al., 2019). Cytokines can directly lower the seizure firing threshold by modulating the function of excitatory and inhibitory neurotransmitter receptors and neuronal ion channels (Vezzani et al., 2019). Elevated neuroinflammatory markers, including **interleukin-1β** (IL-1β) and **tumour necrosis factor-α** (TNF-α), are observed in preclinical models of neonatal seizures and in tissue from patients with elevated neuroinflammation directly linked to epilepsy development (Hagberg et al., 2015; Numis et al., 2019). Importantly, reducing inflammatory signalling has anticonvulsant effects in multiple seizure models (Leavy & Jimenez Mateos, 2020). More specifically, blocking inflammation with the anti-inflammatory drugs **candesartan** and **quercetin** was effective in protecting from neonatal seizures and the resultant brain hyperexcitability in mice and rats, respectively (Quinlan et al., 2019; Wu et al., 2022).

The purinergic **P2X7 receptor** (P2X7R) is a member of the ionotropic **P2X receptor family** (Beamer et al., 2021) that, upon activation by extracellular **adenosine 5'-triphosphate** (ATP), gates the passage of

What is already known

- P2X7 receptor expression is increased in the brain after hypoxia-induced seizures in mouse pups.
- P2X7 receptor antagonists, given before hypoxia, reduce the severity of neonatal seizures in mouse pups.

What does this study add

- P2X7 receptor knockout reduced, whereas P2X7 receptor overexpression exacerbated, seizures in neonatal mice.
- Increased P2X7 receptor expression contributed to unresponsiveness to anti-seizure medication in neonatal seizures.

What is the clinical significance

- Treatment with P2X7 receptor antagonists after hypoxia reduced long-lasting brain hyperexcitability.
- P2X7R-based treatments represent a therapeutic approach for hypoxia-induced neonatal seizures and subsequent development of epilepsy.

cations (e.g., Ca^{2+}, Na^{+} and K^{+}), which leads to **NLRP3** inflammasome activation and IL-1β release (Di Virgilio et al., 2020). Due to its relative low affinity for ATP, P2X7Rs are mainly activated under pathological conditions (Surprenant et al., 1996). Thus, ligands targeting the P2X7R may have fewer effects outside the pathological focus resulting in safer drugs.

Targeting of P2X7Rs has demonstrated efficacy in preclinical models of numerous conditions that have an underlying neuroinflammation, including epilepsy (Beamer et al., 2021). In adult rodents, targeting P2X7Rs was shown to be anticonvulsive and neuroprotective, and to provide disease-modifying effects in epilepsy (Beamer et al., 2017). Regarding neonatal seizures, brain levels of P2X7Rs have been reported to be elevated in mouse pups subjected to hypoxia-induced seizures and in infants with neonatal encephalopathy (NE) (Rodriguez-Alvarez et al., 2017). Furthermore, pre-treatment with P2X7R antagonists modulated seizure severity in a mouse model of neonatal hypoxia (Rodriguez-Alvarez et al., 2017). However, no genetic approaches have been undertaken to determine the contribution of P2X7Rs to neonatal seizures, inflammatory signalling, drug responses and its long-term effects on brain excitability.

By using a hypoxia-induced neonatal seizure model (Rodriguez-Alvarez et al., 2017) and genetically altered mice, we demonstrate that the lack of P2X7Rs at the time of neonatal hypoxia attenuates, whereas overexpression exacerbates, seizures. We further found that P2X7Rs are highly expressed on microglia after hypoxia, that P2X7R deficiency leads to an anti-inflammatory phenotype in microglia, that increased P2X7R expression reduces the responsiveness to ASMs and that targeting P2X7R pharmacologically post-neonatal seizures protects against long-lasting brain hyperexcitability.

2 | METHODS

2.1 | Animals

All animal experiments were performed in accordance with the European Communities Council Directive (2010/63/EU) and approved by the Research Ethics Committee of the Royal College of Surgeons in Ireland (RCSI) (REC1302 and REC202002008) under licence from the Department of Health (AE19127/P013 and AE19127/P064). The animals were treated according to European standards/regulations for animal experiments, and all efforts were made to minimize animal suffering and reduce the numbers of animals under experiments. Animal studies are reported in compliance with the ARRIVE guidelines (Percie du Sert et al., 2020) and with the recommendations made by the *British Journal of Pharmacology* (Lilley et al., 2020). Hypoxia-induced seizure models in rodents have been used extensively to model neonatal seizures and identify potential novel treatments (Leavy & Jimenez Mateos, 2020). Mice represent a valuable experimental model of neonatal seizures for several reasons, including the fact that they share major aspects of brain circuitry with humans, such as the organization and function of the hippocampus. Mice also are large enough to enable multi-channel electroencephalogram (EEG) recordings to score seizures, and they undergo stereotyped behavioural responses during seizures that have human correlates. Another reason for using mice is the availability of numerous transgenic lines to study effects of a specific target gene (e.g., P2X7R knockout [KO] and P2X7R overexpression). For all experiments, we used male and female mice aged between 7 days and 6 weeks. The following mouse strains were used: C57BL/6 OlaHsd wild-type (wt) mice, obtained from the Biomedical Research Facility at RCSI; heterozygous FVB/N-Tg (RP24-114E20-P2X7/StrepHisEGFP) Ani (line 17) BAC transgenic mice, where a full-length *P2rx7* BAC clone tagged to enhanced green fluorescent protein (EGFP) is inserted downstream of the endogenous *P2rx7* to drive overexpression of the P2X7R (P2X7R-OE) (Kaczmarek-Hajek et al., 2018) and the respective wt littermates; and C56BL/6N-P2rx7$^{tm1d(EUKOMM)wtsi}$ P2X7R KO (*P2X7*$^{-/-}$) and respective littermates (*P2X7*$^{+/+}$). Transgenic P2X7R mice were obtained from Annette Nicke, LMU Munich. All transgenic mice were bred to produce both wt and transgenic mice in the same litter. Litters were kept with their dams in a barrier-controlled facility, on a 12 h light/dark cycle, with access to food and water ad libitum. To assess maternal care of dams with either reduced or overexpressed P2X7R levels, Whatman paper (10 g) (Life Sciences, St. Petersburg, FL, USA, Cat #: 10426994) was placed in the cage as nesting material. Unused Whatman paper was weighed once daily for 72 h. All animals were housed in a controlled biomedical facility using Tecniplast conventional cages (Ref. 1284L EUROSTANDARD TYPE II L) and Lignocel BK8/15-25, premium hygienic animal bedding (D0764P00Z) with two to five mice per cage, on a 12 h light/dark cycle at 22 ± 1°C and humidity of 40%–60%, with food and water provided ad libitum. For each cage, enrichment was provided in the form of nesting material (irradiated Bed-r'Nest Brown, Datesand, Item Code CS1BEB), PVC tubes and red polycarbonate mouse houses. All in vivo studies were carried out during the light phase of the cycle. The exact numbers of mice per experimental group are provided in the respective figure legends. The sample size was calculated using G*Power 3.1.9.4 software, with inputs based on data recorded in similar previously performed experiments, to determine suitable sample sizes necessary for detecting differences. Inputs for power analyses in these studies were taken from raw data reported in Engel et al. (2012) and Jimenez-Mateos et al. (2012) (Student's *t* test: Confidence intervals were set at 0.95, giving $\alpha = 0.05$; power was set at $1 - \beta = 0.8$; and the difference between groups ($\mu 1 - \mu 2$) was 35, whereas standard deviation (σ) was 21; using these parameters, a group size of 14 was derived). Animals were euthanized by decapitation for experiments at P7 or via overdose with pentobarbital sodium for experiments exceeding P7 by a trained individual.

2.2 | Neonatal mouse model of hypoxic-induced neonatal seizures

Neonatal seizures were induced as described (Rodriguez-Alvarez et al., 2017) in post-natal (P) 7 mice (weight 4–6 g), an age that has been described to resemble the brain developmental stage of a term

infant (Semple et al., 2013). During the procedure, P7 mouse pups were placed into a clear hypoxic chamber and exposed to global hypoxic conditions of a 95% N_2/5% O_2 premixed gas at 34°C for 15 min. This procedure elicits reliable seizures in 97% of animals, both during and after the hypoxic period (Quinlan et al., 2019). Normoxic controls were placed in the chamber at 21% O_2 (room air) for the same period of time. Hypoxic conditions (5% O_2) were confirmed using the PICO2-OEM optical oxygen meter (PyroScience, Germany). Seizure severity was quantified either via EEG recordings following electrode implantation or in a separate group of mice scoring observable behavioural/clinical seizures. To record seizures electrographically, mice were placed into a stereotaxic frame and anaesthetized with **isoflurane**/oxygen (5% for induction, 2%–3% maintenance) and limited to 10 min of isoflurane exposure. Normal body temperature was maintained via a heat pad (Harvard Apparatus Ltd., UK). The depth of the anaesthesia was frequently tested by checking the plantar nociception or corneal reflex. Additionally, to minimize pain during and after surgery, mice were treated with **buprenorphine** (0.05 mg·kg^{-1}) and EMLA cream (Aspen Pharma, UK), which was applied to head wounds and ear bars. Three partial craniectomies were performed over each temporal cortex (−5 mm AP and ±2.5 mm ML from bregma) and one over the cerebellum. Tethered electrodes (stainless steel screws soldered to a Teflon-insulated stainless steel wire; E/363/20, Bilaney Ltd., UK; diameter: 0.56 mm) were implanted in the burr holes at approximately 1 mm depth, and with great care to avoid damaging the underlying brain surface, then secured with dental cement. The electrode placed over the cerebellum acted as the reference. EEG was recorded via an Xltek digital EEG amplifier and digitalized with a twin software using a notch filter (1 Hz high-pass and 60 Hz low-pass) (Grass Technologies Ltd., Warwick, RI, USA). Following surgery, mice were allowed to recover for 90 min to minimize as much as possible the effect of anaesthetics on seizures. The pups were killed by decapitation after completion of the EEG recordings. In mice without electrode implantation, behavioural/clinical seizures were scored using a 5-point modified Morrison's scale designed to score seizures in neonatal mice (Quinlan et al., 2019): score 0 = normal behaviour; score 1 = immobility/motionless; score 1.5 = immobility, myoclonic jerks and shivers; score 2 = rigid/loss of posture; score 3 = circling, swimming, peddling and tail extension; score 4 = spasms, forelimb tonic-clonic seizures and loss of posture with hyperventilation; and score 5 = score 4 repeatedly. All mice were scored with the researcher blinded to the experimental groups/genotypes.

2.3 | Long-term seizure susceptibility

To investigate the development of an epilepsy-like condition following hypoxia at P7, wt mice were subjected to a seizure challenge using the chemoconvulsant **kainic acid** (KA) (Sigma-Aldrich, Dublin, Ireland), as previously performed (Quinlan et al., 2019). Five weeks after hypoxia (6-week-old mice), mice had three electrodes implanted and secured with dental cement. This implant procedure included two electrodes over each temporal cortex and one as a reference electrode in the cerebellum. To minimize pain during and after surgery, mice were treated with buprenorphine (0.05 mg·kg^{-1}) and EMLA cream (Aspen Pharma, UK), which was applied to head wounds and ear bars. All mice received a single intraperitoneal (i.p.) injection of KA (15 mg·kg^{-1}), which was followed by 90 min of cortical EEG recording in a similar manner to hypoxic seizure studies.

2.4 | Seizure analysis

To analyse EEG recordings, files were uploaded to LabChart reader (V8, ADInstruments Ltd.). EEG total power (μV^2), which is a function of EEG amplitude over time, was analysed by integrating frequency bands from 0 to 60 Hz for hypoxic experiments and 0 to 100 Hz for the seizure susceptibility studies. For these analyses, seizure traces were selected and the values were normalized to the baseline of each animal (pre-hypoxia and pre-KA). The number and duration of seizures (measured as the time from first spike to last spike) were calculated from the EEG recording. Total seizure burden was calculated as the accumulative time that mice were having electrographic polyspike discharges defined as seizures. As in previous studies (Rodriguez-Alvarez et al., 2015), seizures were defined as electrographic polyspike discharges ≥5 Hz, ≥2× baseline EEG amplitude and lasting ≥3 s. Power spectral density heat maps were generated within LabChart (spectral view), with the frequency domain filtered from 0 to 20 Hz and the amplitude domain filtered from 0 to 25 mV.

2.5 | Materials

All drug treatments were delivered via an i.p. injection. Phenobarbital sodium (25 mg·kg^{-1}, 5 ml·kg^{-1}, saline) (Martindale Pharma, Romford, UK) was delivered immediately following hypoxia. **Minocycline** (Sigma-Aldrich, Dublin, Ireland) (30 mg·kg^{-1}, 5 ml·kg^{-1}, dH_2O) was delivered 2 h prior hypoxia. To investigate brain hyperexcitability, i.p. injections of the P2X7R antagonist **JNJ-47965567** (Jimenez-Pacheco et al., 2016) (30 mg·kg^{-1}, 5 ml·kg^{-1}, 30% SBE-β-cyclodextrin) (Janssen R&D, San Diego, CA, USA) begun at P8 24 h after hypoxia and continued once daily for a total of seven injections. Kainic acid was obtained from Sigma-Aldrich (Dublin, Ireland). Drug doses were taken from previously published studies (Beamer et al., 2022; Quinlan et al., 2018; Rodriguez-Alvarez et al., 2017).

2.6 | RNA extraction and qPCR

RNA extraction was performed using the TRizol method, as described before (Alves et al., 2019). Quantity and quality of RNA was measured using a NanoDrop Spectrophotometer (Thermo Scientific, Rockford, IL, USA). Samples with a 260/280 ratio between 1.8 and 2.0 were considered acceptable; 500 ng of total RNA was used to produce complementary DNA (cDNA) by reverse transcription using SuperScript III reverse transcriptase enzyme (Invitrogen, CA, USA) primed

with 50 pmol of random hexamers (Sigma, Dublin, Ireland). Quantitative real-time polymerase chain reaction (qPCR) was performed using the QuantiTect SYBR Green Kit (Qiagen Ltd, Hilden, Germany) and the LightCycler 1.5 (Roche Diagnostics GmbH, Mannheim, Germany). Each reaction tube contained 2 µl cDNA sample, 10 µl QuantiTect SYBR Green Reagent (Qiagen Ltd, Hilden, Germany), 1.25 µM primer pair (Sigma, Dublin, Ireland) and RNAse-free water (Invitrogen, CA, USA) to a final volume of 20 µl. Using LightCycler 1.5 software, data were analysed and normalized to the expression of *β-actin*. Primers used (Sigma, Dublin, Ireland) were as follows: *p2rx7* forward: actggcaggtgtgttccata, reverse: ttggcaagatgtttctcgtg; *p2rx2* forward: atgggattcgaattgacgtt, reverse: gatggtgggaatgagactgaa; *p2rx4* forward: tatgtggtcccagctcagga, reverse: tcacagacgcgttgaatgga; *slc6a1* forward: gctcactctggtttccctct, reverse: caccaacacagaacccaagg; *gria2* forward: actgctctgagaccctgaac, reverse: gagtgttgtgtgctgttcgt; *gfap* forward: agaaaaccgcatcaccattc, reverse: tcacatcaccacgtccttgt; *Iba-1* forward: tggaggggatcaacaagcaa, reverse: accccaagtttctccagcat; *Arc* forward: agcagcagacctgacatcct, reverse: gtgatgcccctttccagacat; and *β-actin* forward: gggtgtgatggtgggaatgg, reverse: ggttggccttagggttcagg.

2.7 | RNA sequencing

RNA sequencing was carried out by omiics.com (Aarhus, Denmark). Mouse hippocampi were removed 24 h after hypoxia (or normoxia) from $P2X7^{+/+}$ and $P2X7^{-/-}$ mouse pups, and RNA was extracted as described above and stored at −80°C. Samples were then shipped to the company and sequenced. Samples were ribosomal RNA (rRNA) depleted and prepared for sequencing using SMARTer Stranded Total RNA Sample Prep Kit—HI Mammalian (Takara). In brief, this kit first removes rRNA using RiboGone technology and specifically depletes nuclear rRNA sequences (5S, 5.8S, 18S and 28S) and mitochondrial rRNA 12S. RiboGone oligos are hybridized to rRNA, which is cleaved using RNase H-mediated cleavage. First-strand synthesis is performed using random priming, adding an anchor for use with later PCR step. Template switching is utilized during the RT step and adds additional non-templated nucleotides to the 3′ end of the newly formed cDNA. PCR is performed by leveraging the non-templated nucleotides and the added anchor sequence to produce Illumina compatible libraries. Prepared libraries were quality controlled using the Bioanalyzer 2100 (Agilent) and qPCR-based concentration measurements. Libraries were equimolarly pooled and sequenced including 20% PhiX in-lane control as 150 bp paired-end reads on an S4 lane of an Illumina NovaSeq 6000 sequencer.

2.8 | Quantification and differential expression analysis

Sequencing data were pre-processed by trimming away low-quality bases with a Phred score below 20, removing adapter sequence and removing the first three nucleotides from reads in fastq file one for each sample, as per kit manufacturer's instructions, using Trim Galore (Version 0.4.1). Quality control was performed using FastQC to ensure high-quality data. Quantification of gene expression was performed by mapping the filtered reads to the mouse genome (mm10) using TopHat2. The software featureCounts was used to quantify the number of reads mapping to each gene using gene annotation from the Gencode M25. Differential expression analysis was performed using DESeq2 in R on the combined gene expression levels. All plotting was done in R. Only protein coding genes were selected for further analyses. Gene expression changes of all conditions are shown in Table S1.

2.9 | Gene Ontology (GO) analysis

Genes with significant ($P < 0.05$) changes in mRNA transcript levels between genotypes ($P2X7R^{+/+}$ vs. $P2X7R^{-/-}$) and treatments (control vs. hypoxia) were analysed by GO terms with the bioinformatic tool DAVID Bioinformatics Resources 6.7.

2.10 | Enrichment analysis

To evaluate whether a gene set is enriched over the background, enrichment analysis studies were carried out using one-sided Fisher's exact test. For our analysis, we used a curated epilepsy-related gene list generated before (Parras et al., 2020). Briefly, this list include genes with mutations that cause pure or relatively pure epilepsies or syndromes with epilepsy as the core symptom (n = 84) (Wang et al., 2017), genes with ultra-rare deleterious variation in familial genetic generalized epilepsy (GGE) and non-acquired focal epilepsy (NAFE) (n = 18) (Epi4K Consortium and Epilepsy Phenome/Genome Project, 2017), and genes localized in loci associated with epilepsy (n = 21) (International League Against Epilepsy Consortium on Complex Epilepsies, 2018).

2.11 | Western blotting

Western blot analysis was performed as described previously (Alves et al., 2019). Lysis buffer (100 mM NaCl; 50 mM NaF; 1% Triton X-100; 5 mM EDTA, pH 8.0; and 20 mM HEPES, pH 7.4) containing a cocktail of phosphatase and protease inhibitors (Sigma-Aldrich, Dublin, Ireland) was used to homogenize hippocampal brain tissue and extract proteins, and concentrations were quantified using a Tecan plate reader at 560 nm; 30 µg of protein samples was loaded onto an acrylamide gel and separated by sodium dodecyl sulfate–polyacrylamide gel electrophoresis (SDS-PAGE). Following electrophoresis, proteins were transferred to a nitrocellulose membrane (GE HealthCare, IL, USA), blocked in 5% milk–Tris-buffered saline–Tween (TBST) and immunoblotted at 4°C overnight with the following primary antibodies prepared in 5% milk–TBST: P2X7R extracellular (1:400; anti-rabbit IgG; Alomone Labs, Jerusalem, Israel; Cat #: APR-008; RRID:AB_2040065), GluR6/7 (1:1000; anti-mouse; Millipore;

Cat #: 04-921; RRID:AB_1587072), GFAP (1:1000; anti-rabbit; Sigma-Aldrich; Cat #: G9269; RRID:AB_477035), $GABA_AR$ (1:1000; anti-mouse; Millipore; Cat #: MABN498; clone N96/55) and Iba-1 (1:400; anti-rabbit; FUJIFILM Wako Chemicals GmbH, Neuss, Germany; Cat #: 019-19741; RRID:AB_839504). Membranes were washed in TBST (10 min) and then incubated with horseradish peroxidase (HRP)-conjugated goat anti-rabbit (1:5000, prepared in 5% milk–TBST; rabbit IgG; HRP; Millipore, MA, USA; Cat #: AP132P; RRID:AB_90264). Membranes were then washed in TBST (3 × 10 min). Protein bands were visualized using FUJIFILM LAS-4000 system with chemiluminescence (Immobilon Western HRP Substrate, Merck Millipore, MA, USA) followed by analysis using Alpha-EaseFC4.0 software. Protein quantity was normalized to the loading control GAPDH (1:1000; anti-rabbit; Cell Signaling Technology). The Immuno-related procedures used comply with the recommendations made by the *British Journal of Pharmacology*.

2.12 | Immunofluorescence and immunohistochemistry

Mice were perfused transcardially with phosphate-buffered saline (PBS, pH 7.4) (5 ml), and brains were removed. Following 24 h of fixation in 4% paraformaldehyde (PFA) at 4°C, brains were transferred to PBS and immersed into 4% agarose; 50 µm sagittal sections were cut using the VT1000S vibratome (Leica Biosystems, Wetzlar, Germany), and sections were stored at −20°C in glycol solution (ethylene glycol [Sigma-Aldrich, Dublin, Ireland], glycerol [Sigma-Aldrich, Dublin, Ireland], 2× phosphate borate and deionized water in a ratio of 3:3:3:1). Tissue sections were incubated with 0.1% Triton/PBS, followed by 1 M glycine and with 1% bovine serum albumin (BSA)–PBS. Sections were then incubated with primary antibodies prepared in 1% BSA–PBS overnight: GFP (1:400; rabbit IgG; Life Science, Dublin, Ireland; Cat #: A11122; RRID:AB_221569), Iba-1 (1:400; goat IgG; Abcam, Cambridge, UK; Cat #: ab5076; RRID:AB_2224402), GFAP (1:400; mouse IgG; Sigma-Aldrich, Dublin, Ireland; Cat #: AB5804; RRID:AB_2109645), NeuN (1:400; Millipore, Cork, Ireland; Cat #: MAB377; RRID:AB_2298772), Olig2 (1:400; mouse; clone 211F1.1; Millipore, Cork, Ireland; Cat #: MABN50; RRID:AB_10807410), CD206 (1:40; goat IgG; R&D Systems, Minneapolis, MN, USA; Cat #: AF2535-SP; RRID:AB_2063012) and CD16/32 (1:100; rat IgG; BD Biosciences, Franklin Lakes, NJ, USA; Cat #:553141; RRID:AB_394656). Diluted primary antibodies were kept at −20°C and re-used up to three times. After washing in PBS, tissue was incubated with fluorescent secondary antibodies, Alexa Fluor 568 (Cat #: A-11011; Cat #: A-11057; and Cat #: A11077) or 488 (Cat #: A11008; Cat #: A21206) (1:400 prepared in 1% BSA–PBS; anti-rabbit IgG; Bio-Sciences, Dublin, Ireland), followed by a short incubation with Hoechst (1:500; Sigma-Aldrich, Dublin, Ireland). FluorSave™ (Millipore, Dublin, Ireland) was used to mount the tissue. Confocal images were taken with a Zeiss 710 LSM NLO confocal microscope equipped with four laser lines (405, 488, 561 and 653 nm) using a 40× oil immersion objective and ZEN 2010B SP1 software.

For double immunofluorescence with Iba-1 (1:200; mouse IgG2a [κ light chain]; Synaptic Systems, Göttingen, Germany; Cat #: 234011; RRID:AB_2884925) and P2X7R (1:200; anti-mouse nanobody; Nolte Group, Hamburg, Germany), stored tissue sections were washed with PBS and blocked with 0.05% saponin/3% BSA/15 mM NH_4Cl/PBS (blocking buffer) for 20 min. Primary antibodies were incubated overnight at 4°C in blocking buffer absent of saponin. After three washes with PBS, sections were incubated for 2 h at room temperature with secondary antibodies, Alexa Fluor 488 and Alexa Fluor 647 (1:400; Life Technologies, Eugene, OR, USA), washed 3× with PBS, shortly stained with DAPI (1 $mg{\cdot}L^{-1}$, Carl Roth, Karlsruhe, Germany), washed with water and mounted (PermaFluor, Thermo Fisher, Dreieich, Germany) for confocal microscopy on a Zeiss LSM880 equipped with four laser lines (405, 488, 561 and 633 nm) using a 40× oil immersion objective and ZEN 2.3 SP1 FP1 (black) software.

2.13 | 3D morphological analysis of microglia

To analyse morphological changes of microglia, immunofluorescence staining was performed as described in the previous section. Microglial cells were identified via Iba-1 (1:400; anti-goat; Abcam, Cambridge, UK). Z-stacks of 0.4 µm between scans (≈50 slices; ≈15 µm thickness) were taken with a Zeiss 710 LSM NLO confocal microscope using a 40× oil immersion objective and ZEN 2010B SP1 software. Z-stacks were taken from each hippocampal subfield (i.e., CA1, CA3 and DG), amounting to three images per slice, n = 3 per group (normoxia) and n = 3 per group (hypoxia) for both $P2X7^{+/+}$ and $P2X7^{-/-}$ mice. Images were subsequently rendered in 3D using FluoRender Version 2.25.0. Three cells from each subfield were selected at random by a reviewer blind to groups and were isolated from the Z-stack. Once isolated, background signal was removed using the 'threshold slider' and volumetric analysis was performed. Cell process length was measured on the same software, using the multipoint measurement tool, beginning from the border of the soma (located using **DAPI**) to the furthest extremity of the cell process. Only primary processes were analysed, meaning processes that extended directly from the soma, as opposed to secondary or tertiary processes branching of the primary cell process. Average process length was calculated as the mean length of all primary processes extending from the cell body of each individual cell. Maximum process length of each isolated cell also was analysed. All measurements were carried out by a researcher blinded to treatment and genotype.

2.14 | Cytokine measurement in brain tissue

Cytokine levels including IL-1β, **IL-6**, TNF-α and **IL-10** were measured using the DuoSet ELISA kits from R&D Systems following the manufacturer's instructions (mouse IL-1β/IL-1F2, Cat #: DY401-05; mouse IL-6, Cat #: DY406; mouse TNF-α, Cat #: DY410-05; and mouse IL-10, Cat #: DY417-05). In a 96-well ELISA plate, the detection antibody was incubated overnight at room temperature. Then, 100 µl of

the samples (50 ng) and standard curve (IL-1β and IL-6: from 15.6 to 1000 pg·ml^{-1}; TNF-α and IL-10: 31.2–2000 pg·ml^{-1}) were added to the wells and incubated for 2 h at room temperature, followed by incubation with 100 µl of detection antibody and incubated for 2 h at room temperature. Then, 100 µl of streptavidin–HRP complex was added to the wells followed by 45 min incubation in the dark. A colour reaction, caused by the addition of a substrate solution (100 µl) and terminated by a stopping solution (50 µl), was quantified at 450 and 570 nm using a microplate reader. The cytokine concentration was obtained following the manufacturer's recommendations; 570 nm values were subtracted from the 450 nm values. The $\log_{10}$ of the standard curve values was plotted, and a line of best fit was generated. The amount of cytokines was extrapolated using a standard curve and taking the average of calculated triplicates. Cytokine concentration was then normalized to milligrams of total protein concentration in tissue. Data are presented as n-fold of control samples.

2.15 | Fluoro-Jade B (FjB) staining

To assess P2X7R antagonist-induced neurodegeneration, FjB staining was carried out as before using brain slices from mice treated with the P2X7R antagonist JNJ-47965567 for 7 days starting at P8 until P14 (Engel et al., 2018). Briefly, 30 µm coronal sections were cut on a vibratome. Once mounted on glass slides, tissue sections were fixed in 4% PFA, rehydrated in ethanol and then transferred to a 0.006% potassium permanganate solution followed by incubation with 0.001% FjB (Chemicon Europe Ltd, Chandler's Ford, UK). Sections were mounted in Dibutylphthalate Polystyrene Xylene (DPX) mounting solution (Sigma-Aldrich, Dublin, Ireland).

2.16 | Experimental design and statistical analysis

All experiments were carried out using both male and female mice, with the corresponding littermates. The data and statistical analysis comply with the recommendations of the *British Journal of Pharmacology* on experimental design and analysis in pharmacology (Curtis et al., 2022). All experiments were designed to generate groups of equal size, using randomization and blinded analysis. To reduce unwanted sources of variation in our EEG analysis, the data were normalized to baseline or control groups if not indicated otherwise. Group size is the number of independent values, and statistical analysis was done using these independent values. Outliers were included in data analysis and presentation. In multigroup studies with parametric variables, post hoc tests were conducted only if *F* in ANOVA (or equivalent) achieved the 'chosen' necessary level of statistical significance and there was no significant variance in homogeneity. All datasets were tested for normal distribution and homogeneity of variance to confirm that non-parametric testing was not required. Statistical design for experiments can be found in the 'Results' section in figure legends including control groups, group size and statistical test used. Statistical analysis of data was carried out using GraphPad Prism 5 and StatView software (SAS Institute, Cary, NC, USA). Data are presented as means ± standard error of the mean (SEM). One-way ANOVA parametric statistics with post hoc Fisher's protected least significant difference test was used to determine statistical differences between three or more groups. Unpaired two-tailed Student's *t* test was used for two-group comparison. Two-way ANOVA was used for repeated measures between groups where a series of measurements have been taken from the same mouse at different time points. Statistical analysis was undertaken only for studies where each group size was at least n = 5. Significance was accepted at $^*P < 0.05$.

2.17 | Nomenclature of targets and ligands

Key protein targets and ligands in this article are hyperlinked to corresponding entries in http://www.guidetopharmacology.org and are permanently archived in the Concise Guide to PHARMACOLOGY (Alexander et al., 2021).

3 | RESULTS

3.1 | P2X7R deficiency reduces seizure severity after hypoxia in neonates

To obtain genetic proof of an involvement of the P2X7R in neonatal seizures, P7 P2X7R-deficient mouse pups were subjected to global hypoxic conditions (Figure 1a). Quantitative PCR analysis confirmed the absence of P2X7R expression in the hippocampus (Figure 1b). Hippocampal mRNA levels of ***P2rx4*** and ***P2rx2*** were not significantly altered in *P2X7*$^{-/-}$ mice. No changes could be observed between genotypes when analysing ***GRIA2*** (glutamate ionotropic receptor AMPA-type subunit 2), ***SLC6A1*** (γ-aminobutyric acid [GABA] transporter type 1) and *Arc* (Activity-regulated cytoskeleton-associated protein: a marker of neuronal activity) (Figure 1b). In addition, similar transcript levels were found in the hippocampus for the inflammation markers *Iba-1* (ionized calcium-binding adapter molecule 1) and *GFAP* (glial fibrillary acidic protein) between genotypes (Figure 1c). Likewise, hippocampal cytokine levels were similar between groups, including the pro-inflammatory cytokine IL-1β and the anti-inflammatory cytokine IL-10 (Figure 1d). Maternal care from heterozygous P2X7R breeding trios was similar to wt mice, as shown by similar nest building (Figure S1a). Basal weight of P7 mouse pups also was similar across genotypes (Figure S1b).

Next, we characterized the seizure phenotype in P2X7R-deficient mice (*P2X7*$^{+/-}$ and *P2X7*$^{-/-}$). During the hypoxic period, all genotypes had similar seizure behaviours (Figure 1e). However, in contrast to *P2X7*$^{+/+}$ and *P2X7*$^{+/-}$ mice, *P2X7*$^{-/-}$ mice had significantly less severe seizures after hypoxia (Figure 1e). Next, using EEG recording from cortical implanted electrodes in a separate set of mice, we confirmed these results with *P2X7*$^{-/-}$ mice having a shorter average seizure duration, reduced number of seizures and a reduced time spent in seizures in the post-hypoxic period (Figure 1f). Of note, in contrast

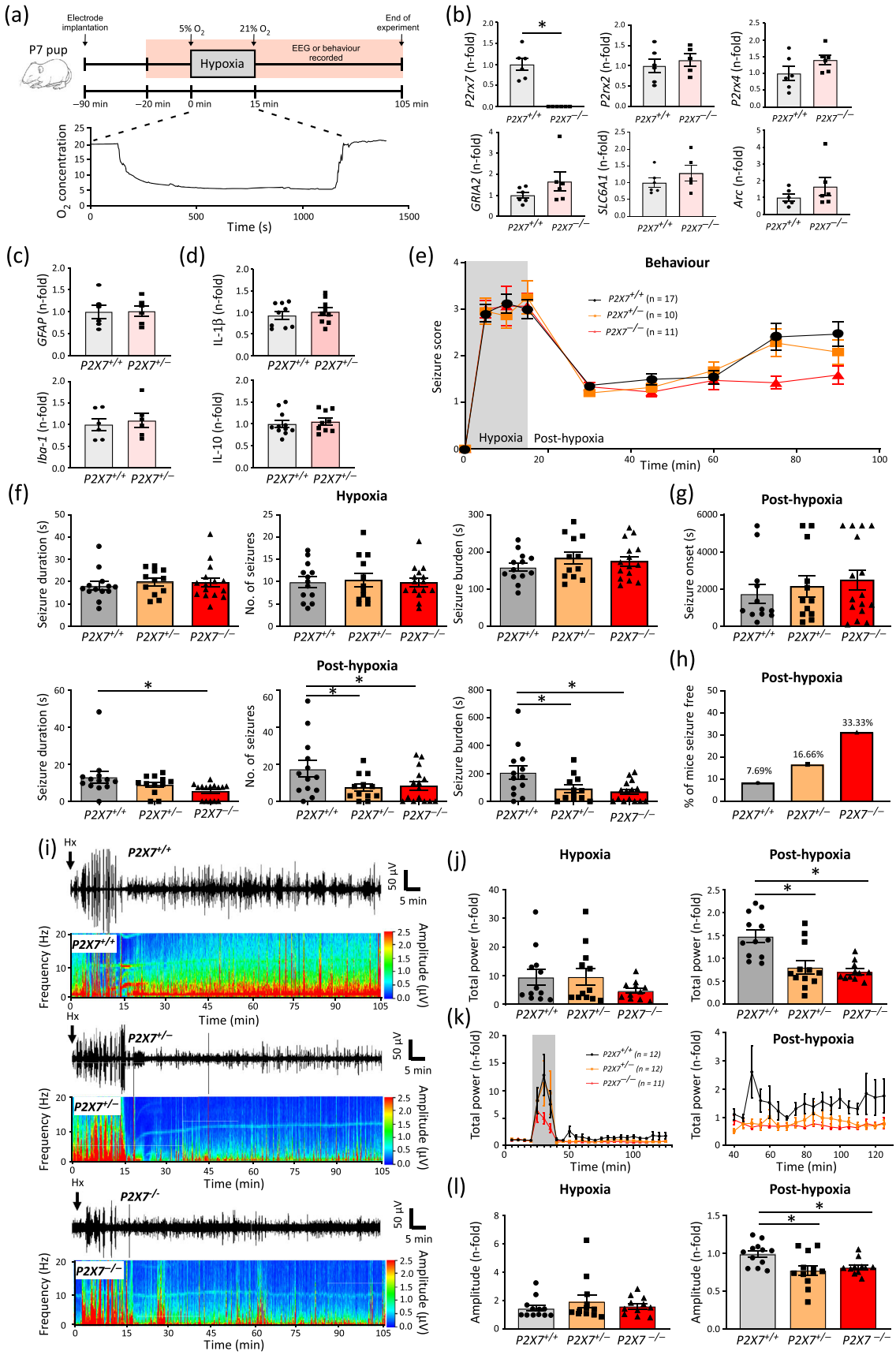

FIGURE 1 Legend on next page.

to behavioural seizures, *P2X7*$^{+/-}$ showed a reduced electrographic seizure phenotype after hypoxia (Figure 1f). The onset of first seizure after hypoxia was similar across genotypes (Figure 1g). However, although 7.69% of *P2X7*$^{+/+}$ mice did not present with seizures following hypoxia, 16.66% of *P2X7*$^{+/-}$ and 33.33% of *P2X7*$^{-/-}$ mice did not present with EEG-confirmed seizures after hypoxia (Figure 1h). Analysis of total seizure power confirmed the significant reduction of seizure activity in P2X7R-deficient mice during the post-hypoxic period. No significant difference in seizure severity between genotypes was observed during hypoxia (Figure 1i–k). Likewise, *P2X7*$^{+/-}$ and *P2X7*$^{-/-}$ mice showed a reduced amplitude after hypoxia (Figure 1l).

3.2 | Increased P2X7R expression contributes to neonatal seizures after hypoxia and reduces responsiveness to phenobarbital

To test whether P2X7R-OE impacts on seizures or responsiveness to ASMs, we used P7 mouse pups overexpressing the P2X7R (P2X7R-OE) (Kaczmarek-Hajek et al., 2018) (Figure 2a). Hippocampal protein levels of the P2X7R were roughly doubled in P2X7R-OE mice, whereas protein levels of microglia and major receptors of both the GABAergic and glutamatergic neurotransmitter systems were unchanged (Figure 2b). Hippocampal RNA levels of *P2rx2* and *P2rx4* genes also were unchanged between genotypes. P2X7R-OE mice showed, however, increased *Arc* expression (Figure 2c). No significant differences in the cytokines IL-1β and IL-6 and TNF-α were observed between genotypes (Figure 2d). P2X7R-OE had no impact on maternal care (Figure S1c) or body weight (Figure S1d).

When subjecting P7 P2X7R-OE mouse pups to hypoxia, we observed an increase in the seizure behaviour in mice overexpressing the P2X7R in the post-hypoxic period, with the greatest differences occurring 45–60 min after normal O_2 concentrations were reinstated. No significant differences were observed during hypoxia (Figure 2e). EEG recordings showed that P2X7R-OE pups had an increased average seizure duration and seizure burden during and after hypoxia (Figure 2f). Although seizure onset was similar between genotypes after hypoxia (Figure 2g), all P2X7R-OE mice experienced seizures after hypoxia, in contrast to wt mice where 18% of mice remained seizure free (Figure 2h). Furthermore, total power was increased in P2X7R-OE mice during and after hypoxia (Figure 2i–k). Although slightly increased in P2X7R-OE mice, no significant change in EEG amplitude was observed between genotypes (Figure 2l).

To test whether P2X7R-OE increases unresponsiveness to ASMs during neonatal seizures, wt and P2X7R-OE mouse pups were treated with phenobarbital immediately after hypoxia (Figure 3a). Although phenobarbital was effective in suppressing post-hypoxic seizures in ~78% of wt mice, phenobarbital could only suppress seizures in 15% of P2X7R-OE mice (Figure 3b). As before, vehicle-treated P2X7R-overexpressing mice showed a tendency towards a higher seizure burden when compared to vehicle-treated wt mice when subjected to hypoxia (Figure 3c). Although phenobarbital was able to reduce seizure burden in wt mice, this effect was much less accentuated in P2X7R-OE mice, with phenobarbital-treated P2X7R-OE mice presenting a higher seizure burden when compared to phenobarbital-treated wt littermates (Figure 3c).

3.3 | P2X7R effects on neonatal seizures are mediated via inflammation

To visualize P2X7R cell type-specific localization following hypoxia, we used our P2X7R-OE mice and a highly specific P2X7R nanobody to confirm our results in wt mice (Kaczmarek-Hajek et al., 2018). GFP-positive cells colocalized predominantly with microglia positive for Iba-1 in wt normoxic control mice. This staining pattern was consistent at 24 and 72 h after hypoxia in the cortex and all hippocampal subfields analysed (Figure 4a). When we investigated oligodendroglial

FIGURE 1 Reduced seizure severity in P2X7R-deficient mouse pups during and following hypoxia. (a) Experimental design of neonatal seizure model. Mouse pups (P7) were subjected to hypoxia (5% O_2) for 15 min. If EEG was recorded, EEG screws were implanted 90 min before hypoxia and EEG recordings commenced 20 min before hypoxia (baseline). EEG recording continued for an additional 90 min after hypoxia. Behavioural changes during hypoxia and after hypoxia were scored in a separate group of mice. Bottom schematic shows representative O_2 trace during hypoxia. (b) Hippocampal mRNA expression of *P2rx7* is absent in *P2X7*$^{-/-}$ P7 mouse pups (unpaired Student's *t* test; n = 6 per group). No difference in hippocampal mRNA levels of *P2rx4*, *P2rx2*, *GRIA2*, *SLC6A1* and *Arc* between *P2X7*$^{+/+}$ and *P2X7*$^{-/-}$ P7 mouse pups (n = 6 per group). Data were normalized to *β-actin*. (c) No difference was observed in hippocampal mRNA levels of the inflammatory markers *GFAP* and *Iba-1* between *P2X7*$^{+/+}$ and *P2X7*$^{-/-}$ P7 mouse pups (n = 6 per group). Data were normalized to *β-actin*. (d) No difference was observed in hippocampal cytokine levels for IL-1β and IL-10 between *P2X7*$^{+/+}$ and *P2X7*$^{-/-}$ P7 mouse pups (n = 11 [*P2X7*$^{+/+}$] and 9 [*P2X7*$^{-/-}$]). (e) Graph showing behavioural seizure scores during hypoxia and after hypoxia in P7 mouse pups (*P2X7*$^{+/+}$, *P2X7*$^{+/-}$ and *P2X7*$^{-/-}$) (two-way ANOVA with Tukey's multiple comparisons; n = 17 [*P2X7*$^{+/+}$], 10 [*P2X7*$^{+/-}$] and 11 [*P2X7*$^{-/-}$]). (f) Graphs showing EEG-recorded seizure duration, number of seizures and seizure burden during hypoxia and after hypoxia (one-way ANOVA with Fisher's post hoc test; n = 13 [*P2X7*$^{+/+}$], 12 [*P2X7*$^{+/-}$] and 15 [*P2X7*$^{-/-}$]). (g) Graph showing time to first seizure following hypoxia (n = 13 [*P2X7*$^{+/+}$], 12 [*P2X7*$^{+/-}$] and 15 [*P2X7*$^{-/-}$]). (h) Graph showing percentage of mice that are seizure free during the post-hypoxic period (90 min EEG recording) (n = 13 [*P2X7*$^{+/+}$], 12 [*P2X7*$^{+/-}$] and 15 [*P2X7*$^{-/-}$]). (i) Representative EEG traces and heat maps of frequency and amplitude data starting at the time of hypoxia until 90 min after hypoxia. Of note, reduced seizure severity was seen in P2X7R-deficient mouse pups. (j) Graphs showing total seizure power during hypoxia (15 min EEG recording) and after hypoxia (90 min EEG recording) (one-way ANOVA with Fisher's post hoc test; n = 12 [*P2X7*$^{+/+}$], 12 [*P2X7*$^{+/-}$] and 11 [*P2X7*$^{-/-}$]). (k) Graphs showing total power on the EEG during hypoxia (15 min EEG recording) and after hypoxia (90 min EEG recording) over time when analysed every 5 min (n = 12 [*P2X7*$^{+/+}$], 12 [*P2X7*$^{+/-}$] and 11 [*P2X7*$^{-/-}$]). (l) Amplitude of EEG traces during 20 min of hypoxia and after hypoxia (90 min) (ANOVA with Fisher's post hoc test [after hypoxia]; n = 12 [*P2X7*$^{+/+}$], 12 [*P2X7*$^{+/-}$] and 11 [*P2X7*$^{-/-}$]). *$P < 0.05$.

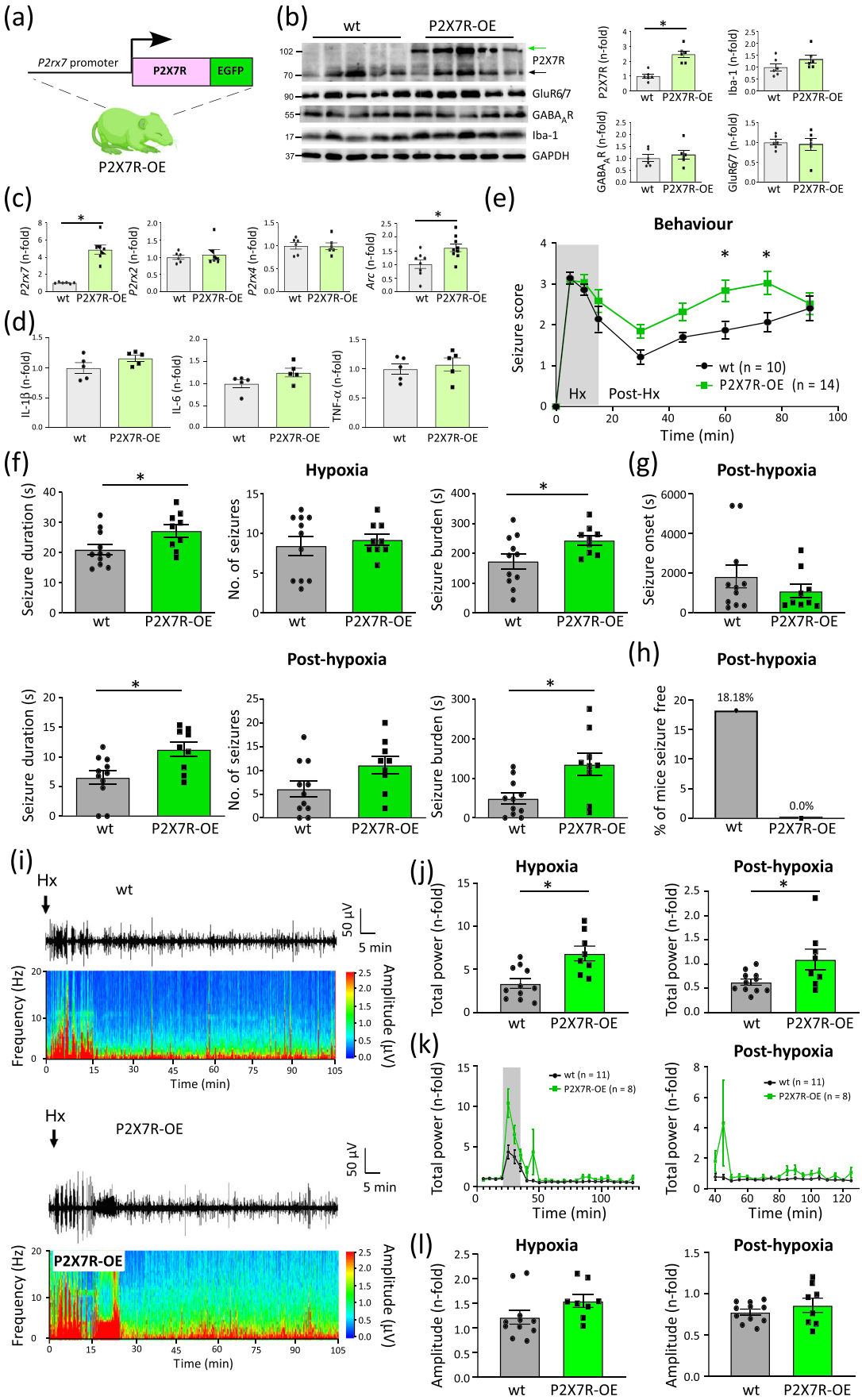

FIGURE 2 Legend on next page.

P2X7R expression, we observed GFP-positive cells colocalizing with Olig2-positive cells in P2X7R-OE mouse pups without hypoxia in both the hippocampus and cortex (Figure 4b). Interestingly, GFP colocalization with Olig2 was reduced 24 h after hypoxia in the hippocampus and cortex, yet was reinstated 72 h after hypoxia (Figure 4b). GFP did not colocalize with NeuN-positive cells in the cortex or any hippocampal subfield under any condition (Figure 4c). Likewise, no colocalization of GFP with GFAP-positive cells was observable across all conditions in the cortex and hippocampus (Figure 4d). Staining of brain slices from wt mouse pups subjected to hypoxia with P2X7R-detecting nanobodies confirmed the mainly microglial P2X7R localization under physiological conditions and 24 h after hypoxia (Figure 4e). Nanobody signal was absent in slices obtained from P7 *P2X7*$^{-/-}$ mouse pups (Figure 4f). Nanobody signal also was found to colocalize strongly with GFP signal in P2X7R-OP mice (Figure 4g).

To test whether P2X7R contributes to seizures via its effects on inflammation, wt and P2X7R-OE mice were pre-treated with minocycline 2 h before hypoxia (Figure 5a). No difference in seizure severity was observed between P2X7R-OE mice and wt mice, when mice were pre-treated with minocycline (Figure 5b). We then investigated whether P2X7R signalling during hypoxia impacts on the activation state of microglia. Here, double immunostaining for the microglial marker Iba-1 and the pro-inflammatory marker **CD16** showed an elevation of CD16-positive cells in the hippocampus of *P2X7*$^{+/+}$ mice 24 h after hypoxia not observed in *P2X7*$^{-/-}$ mice (Figure 5c). In contrast, double staining for Iba-1 and the anti-inflammatory microglial marker CD206 (C-type mannose receptor 1) showed an increase of CD206-positive cells in *P2X7*$^{-/-}$ mice 24 h after hypoxia not observed in *P2X7*$^{+/+}$ mice (Figure 5d). In addition, we found no gross differences between wt and *P2X7R*$^{-/-}$ mice under normoxic control conditions with microglia from both genotypes showing similar volumes of both soma and whole cell bodies including all microglial processes (Figure S2). Hypoxia led, however, to a slightly larger soma/volume ratio in *P2X7*$^{+/+}$ mice (Figure S2). In contrast, microglia from *P2X7*$^{-/-}$ mouse pups obtained 24 h after hypoxia showed slightly more primary processes than those from wt mice subjected to hypoxia (Figure S2), consistent with a less activated and less inflammatory phenotype. Furthermore, following hypoxia, microglia in *P2X7*$^{+/+}$ mice had a slightly decreased average primary process length and maximum primary process length. No decreases were evident in *P2X7*$^{-/-}$ mice following hypoxia (Figure S2).

3.4 | P2X7R antagonism reduces long-lasting brain hyperexcitability following hypoxia in neonates

To test whether P2X7R antagonism impacts on long-lasting brain hyperexcitability after hypoxia, mice were treated 24 h after hypoxia with the P2X7R antagonist JNJ-47965567 (30 mg·kg^{-1}) or vehicle daily for 7 days. At 5 weeks after hypoxia, mice were subjected to a seizure susceptibility test using a low dose of KA (15 mg·kg^{-1}) (Figure 6a). When subjected to i.p. KA at 6 weeks of age, vehicle-treated mice subjected to hypoxia at P7 had a more severe seizure phenotype when compared with mice that had not experienced seizures as neonates (Figure 6b–d). In contrast, mice subjected to hypoxia-induced seizures, but treated with the P2X7R antagonist, had significantly less severe seizures when compared with vehicle-treated mice subjected to hypoxia, similar to vehicle-treated control mice (Figure 6b–d). P2X7R antagonist treatment had no effect on body weight and did not cause obvious neurodegeneration in the brain (Figure S3a–c).

3.5 | Identification of P2X7R regulated pathways during normal physiology and after hypoxia in neonates

To investigate P2X7R-dependent gene changes after hypoxia, hippocampi from *P2X7*$^{+/+}$ and *P2X7*$^{-/-}$ mice were analysed via RNA sequencing 24 h after control normoxic or hypoxic conditions

FIGURE 2 Overexpression of the P2X7R worsens the hypoxia-induced seizure phenotype. (a) Schematic showing transgenic approach to overexpress the P2X7R. Transgenic P2X7R is C-terminally fused to the fluorescent protein EGFP and expressed under the transcriptional control of the BAC-derived *P2rx7* promoter. (b) Graphs and representative western blots of hippocampal samples showing increased P2X7R expression in P7 P2X7R-OE mouse pups. Band at 72 kDa corresponds to endogenous P2X7R and band at 102 kDa to P2X7R fused to EGFP (unpaired Student's *t* test; n = 6 per group). No changes between genotypes in hippocampal protein levels of GluR6/7, $GABA_AR$ and Iba-1 (n = 6 per group). (c) Graph showing increased hippocampal *P2rx7* mRNA levels in P2X7R-OE P7 mouse pups (unpaired Student's *t* test; n = 6 per group). No changes between genotypes in *P2rx2* and *P2rx4* (n = 6 per group). Increased *Arc* mRNA levels in P2X7R-OE mouse pups (unpaired Student's *t* test; n = 8 per group). (d) Graph showing levels of hippocampal cytokines IL-1β, IL-6 and TNF-α in P7 P2X7R-OE and wt mouse pups (n = 5 per group). (e) Graph showing behavioural seizure scores of wt and P2X7R-OE P7 mouse pups during hypoxia (grey highlight, 15 min) and after hypoxia (90 min) (two-way ANOVA with Tukey's multiple comparisons; n = 11 [wt] and 14 [P2X7R-OE]). (f) Graph showing EEG-recorded seizure duration, number of seizures and seizure burden in P7 wt and P2X7R-OE mouse pups during hypoxia (15 min) and after hypoxia (90 min) (unpaired Student's *t* test; n = 11 [wt] and 9 [P2X7R-OE]). (g) No difference was observed in the onset to first seizure after hypoxia between wt and P2X7R-OE mice (n = 11 [wt] and 9 [P2X7R-OE]). (h) Percentage of mice showing seizures during the post-hypoxic period (90 min) starting from the time of reoxygenation (n = 11 [wt] and 9 [P2X7R-OE]). (i) Representative EEG traces and heat maps starting at the time of hypoxia of both wt and P2X7R-OE mice. Of note, increased seizure severity in P2X7R-OE mouse pups. (j) Graphs showing EEG total power of wt and P2X7R-OE P7 mouse pups during hypoxia (15 min) and after hypoxia (90 min) (unpaired Student's *t* test; n = 11 [wt] and 8 [P2X7R-OE]). (k) Graphs showing EEG total power over time during hypoxia (grey highlighted) and after hypoxia measured every 5 min of wt and P2X7R-OE mouse pups (n = 11 [wt] and 8 [P2X7R-OE]). (l) Graphs showing EEG amplitude of wt and P2X7R-OE P7 mouse pups during hypoxia (15 min) and after hypoxia (90 min) (unpaired Student's *t* test; n = 11 [wt] and 8 [P2X7R-OE]). *$P < 0.05$.

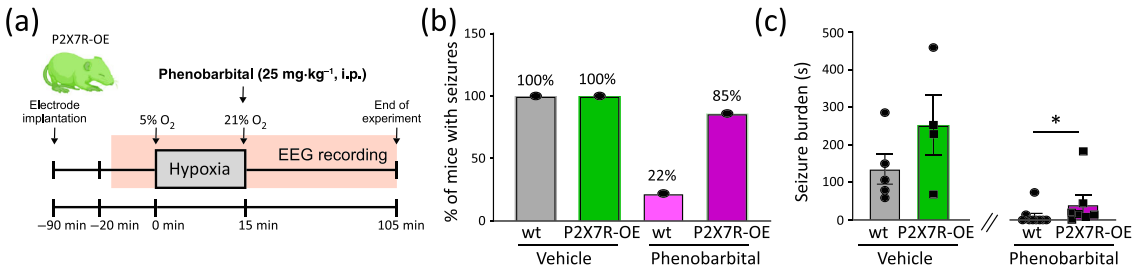

FIGURE 3 Overexpression of P2X7R decreases the responsiveness of P7 mice to phenobarbital treatment during hypoxia. (a) Schematic outlining experimental paradigm, with phenobarbital (25 mg·kg^{-1}) injected directly following hypoxia. (b) Percentage of wt and P2X7R-OE P7 mouse pups showing seizure activity after treatment with vehicle or phenobarbital. EEG was recorded for 90 min starting at the time of reoxygenation (vehicle: n = 5 [wt] and 4 [P2X7R-OE]; phenobarbital: n = 9 [wt] and 7 [P2X7R-OE]). (c) Graph showing EEG-recorded seizure burden (90 min) of wt and P2X7R-OE P7 mouse pups following both vehicle and phenobarbital treatment (unpaired Student's *t* test; phenobarbital: n = 9 [wt] and 7 [P2X7R-OE]). *$P < 0.05$.

(Figure 7a). Under non-hypoxic control conditions, 517 genes were differentially expressed between genotypes (305 up-regulated and 211 down-regulated) (Figure 7b) (Table S2 shows the 25 top up- and down-regulated genes in *P2X7*$^{-/-}$ mice under normoxic control conditions); 2245 genes were found significantly dysregulated between genotypes after hypoxia (1188 up-regulated and 1057 down-regulated) (Figure 7b) (Table S3 shows the 25 top up- and down-regulated genes in *P2X7*$^{-/-}$ mice after hypoxia). Differences between genotypes were higher, particularly after hypoxia, when compared to changes observed between normoxia and hypoxia in wt mice. The average fold change of genes dysregulated under normoxic control conditions in *P2X7*$^{-/-}$ mouse pups was lower when compared to fold changes after hypoxia (Figure 7c).

Genes up-regulated after hypoxia in *P2X7*$^{+/+}$ mice (115 genes) were distinct to those up-regulated in *P2X7*$^{-/-}$ mice after hypoxia (245 genes) (Figure 7d). Among the down-regulated pool following hypoxia, only two genes (*Clic4* and *Mdm4*) were commonly down-regulated between genotypes; 157 genes were down-regulated in *P2X7*$^{+/+}$ mice and 246 genes in *P2X7*$^{-/-}$ mice in post-hypoxic conditions. Interestingly, genes involved in transcription (*Tfdp2* and *Rfx4*) were up-regulated in *P2X7*$^{+/+}$ whilst simultaneously being down-regulated in *P2X7*$^{-/-}$ mice. Three genes (*Hcfc1r1*, *Babam1* and *Prdx5*) were down-regulated in *P2X7*$^{+/+}$ mice whilst being up-regulated in *P2X7*$^{-/-}$ mice after hypoxia (Figure 7d). However, when we focused on gene changes between genotypes, 99 genes were commonly up-regulated in *P2X7*$^{-/-}$ mice in both normoxic and post-hypoxic mice (e.g., *Uba52*, *Kxd1*, *Triobp* and *Midn*) and 69 genes were commonly down-regulated (e.g., *Mal2*, *Ccn3*, ***Hcn1*** and *Glrb*), whereas only 8 genes were differentially expressed in opposite directions between conditions (Figure 7e). Notably, we found a very significant enrichment of up- and down-regulated genes between conditions, indicating that gene expression changes are preserved in *P2X7*$^{-/-}$ mice regardless of pathological background (Figure 7f).

GO analyses revealed that, under normoxic control conditions, pathways up-regulated in *P2X7*$^{-/-}$ mice included those involved in cell proliferation and differentiation, inflammatory pathways, and pathways involved with the cholinergic synapse. Pathways down-regulated in *P2X7*$^{-/-}$ under normoxic control conditions included those involved with the glutamatergic synapse, thermogenesis and metabolism (Figure 7g and Table S4). In contrast to normoxic conditions, 'oxidative phosphorylation' and 'thermogenesis' pathways were up-regulated in *P2X7*$^{-/-}$ mice following hypoxia. Other notable pathways up-regulated were the '**VEGF signalling** pathway' and '**HIF-1 signalling** pathway', previously described as protective responses to hypoxic conditions (Feng et al., 2008). Pathways involved in protein degradation and removal of cellular debris (e.g., 'ubiquitin-mediated proteolysis' and 'autophagy') were down-regulated in *P2X7*$^{-/-}$ mice after hypoxia. Other down-regulated pathways included those affecting neurotransmitter systems ('glutamatergic synapse' and 'GABAergic synapse'), 'TGF-β signalling pathway' and 'mTOR signalling pathway' (Figure 7h and Table S4).

To investigate whether P2X7R deficiency impacts on the expression of known epilepsy-related genes, we compared our dataset to previously published epilepsy-related gene lists. Here, we observed that dysregulated genes in *P2X7*$^{-/-}$ mice showed an almost twofold enrichment of epilepsy-related genes within the down-regulated gene pool both under control and hypoxic conditions (Figure 7i and Table S5).

4 | DISCUSSION

Here, we provide genetic proof of an involvement of P2X7R in the generation of seizures after hypoxia in neonates. We further provide evidence that increased P2X7R expression in microglia contributes to drug unresponsiveness and that P2X7R antagonism reduces hypoxia-induced brain hyperexcitability.

Treatment for neonatal seizures remains a clinical challenge, with current ASMs being effective in ~50% of patients (Wagner et al., 2021). Other strategies, including therapeutic hypothermia, are effective in treating hypoxia, yet its ability to reduce seizures is less conclusive (Hellstrom-Westas et al., 2015). Previous research has suggested that P2X7Rs are involved in neonatal seizures, with P2X7R expression observed to be up-regulated in brain tissue of mouse pups

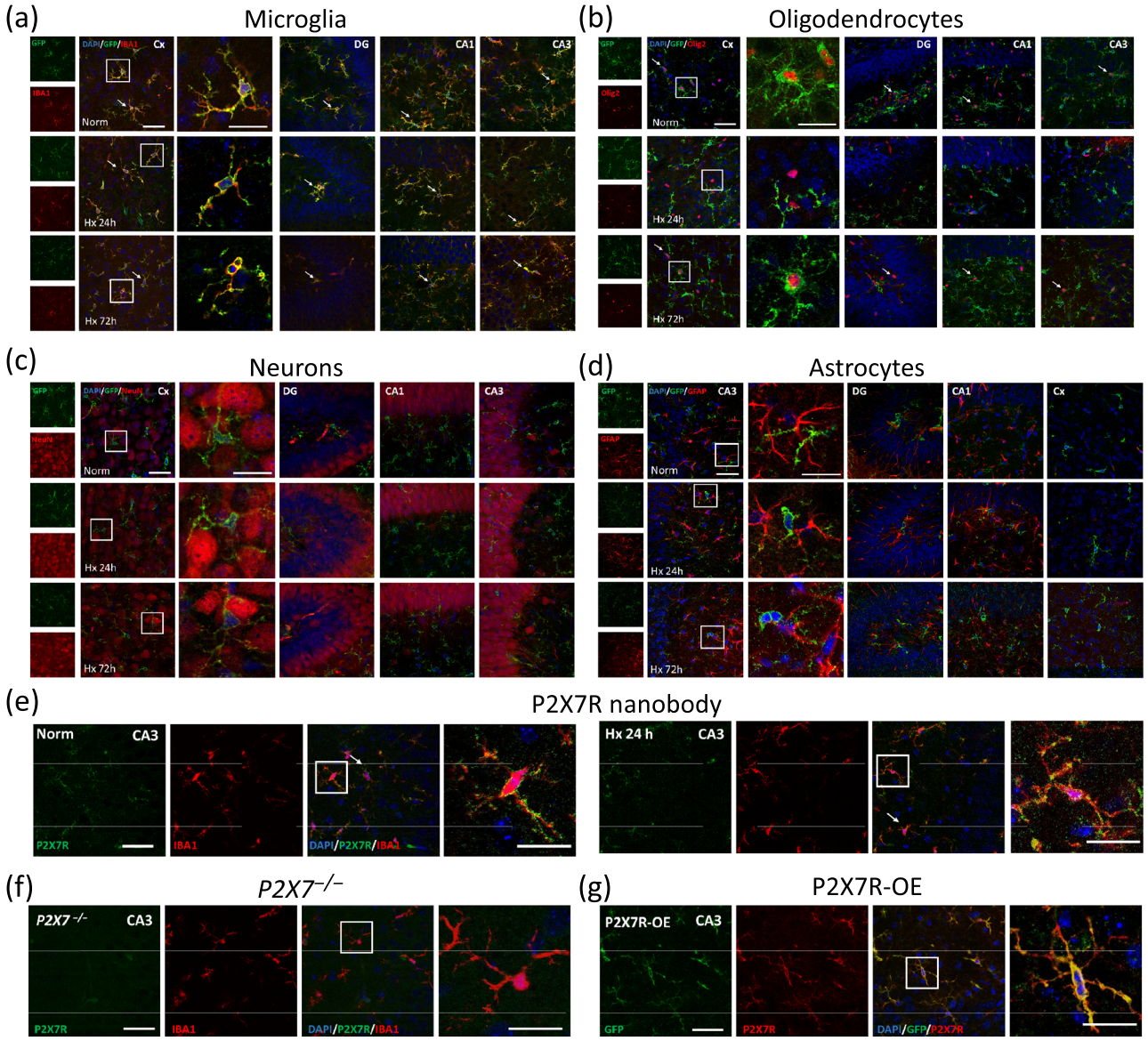

FIGURE 4 Cell type-specific expression of the P2X7R during physiological control conditions and following hypoxia in neonates. (a) Representative images of brain slices taken from P2X7R-OE P7 mouse pups under normoxic control conditions and 24 and 72 h after hypoxia stained for Iba-1 (red) and GFP (green) from the cortex (Cx), dentate gyrus (DG), cornu ammonis 1 (CA1) and cornu ammonis 3 (CA3). (b) Representative images of different brain regions from P2X7R-OE mouse pups against GFP (green) and Olig2 (red) under control conditions and 24 and 72 h after hypoxia. Of note, GFP–Olig2 colocalization is no longer apparent 24 h after hypoxia. GFP–Olig2 colocalization is, however, restored 72 h after hypoxia. (c) Representative images showing no colocalization of GFP (green) with NeuN (red) in any of the brain regions selected nor at any treatment (i.e., normoxia and hypoxia). (d) Representative images showing no colocalization of GFP (green) with GFAP (red) in any of the brain regions selected nor at any treatment (i.e., normoxia and hypoxia). (e) Representative images from wt mice sections stained with the P2X7R nanobody. Colocalization of the P2X7R nanobody (green) with Iba-1 (red) in the CA3 region is observed in both control and 72 h after hypoxia. (f) Representative images from P7 *P2X7*$^{-/-}$ mouse pups showing absence of P2X7R nanobody signal. (g) Representative images from P7 P2X7R-OE mouse pups showing colocalization of GFP (green) with P2X7R nanobody (red). Arrows indicate colocalization. Square indicates selected cell that is enlarged. Scale bar = 50 μm, enlarged 25 μm.

subjected to hypoxia and in infants who died of neonatal encephalopathy (NE). Further evidence stems from anticonvulsive effects of P2X7R antagonists when administered before hypoxia in P7 mice (Rodriguez-Alvarez et al., 2017). We now extend these data by providing genetic proof of an involvement of P2X7R to seizure generation, drug refractoriness and long-term consequences of neonatal seizures. We further provide evidence of how P2X7Rs contribute to seizures and subsequent pathology with its effects on neuroinflammatory processes being the most likely mechanism.

Our data show P2X7Rs to be highly expressed in microglia under physiological conditions and after hypoxia. This is consistent with its well-recognized role in microglia (Monif et al., 2009). Similar to adults

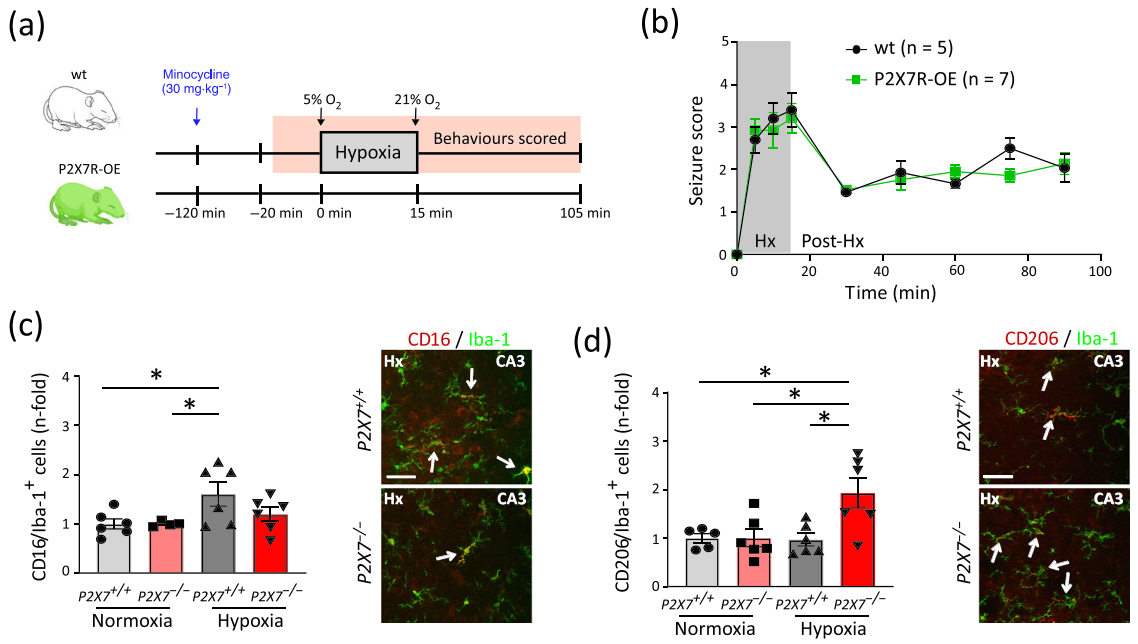

FIGURE 5 P2X7R-dependent effects on seizures are mediated via inflammation. (a) Schematic of the experimental paradigm, with both wt and P2X7R-OE P7 mouse pups injected with minocycline (30 mg·kg^{-1}) 2 h before the induction of hypoxia. (b) No increase in behavioural seizure score was observed between P2X7R-OE and wt mice after minocycline injection, both during hypoxia (grey highlight) and during the post-hypoxic period (n = 5 [wt] and 7 [P2X7R-OE]). (c) Graph and representative images showing CD16/Iba-1-positive cells in the hippocampus of *P2X7*$^{+/+}$ and *P2X7*$^{-/-}$ P7 mouse pups subjected to normoxic control conditions and 24 h after hypoxia (one-way ANOVA with Fisher's post hoc test; n = 6 per group). Data were normalized to normoxic control conditions. Arrows indicate colocalization. Scale bar = 50 μm. (d) Graph and representative images showing CD206/Iba-1-positive cells in the hippocampus of *P2X7*$^{+/+}$ and *P2X7*$^{-/-}$ P7 mouse pups subjected to normoxic control conditions and 24 h after hypoxia (one-way ANOVA with Fisher's post hoc test; n = 6 per group). Arrows indicate colocalization. Scale bar = 50 μm. Data were normalized to normoxic control conditions. Arrows indicate colocalization. *P < 0.05.

(Morgan et al., 2020), P2X7Rs were not detected on astrocytes or on neurons. P2X7Rs were, however, detected on oligodendrocytes. Why P2X7R expression decreases on oligodendrocytes after hypoxia remains to be determined. P2X7Rs have, however, been shown to promote oligodendrocyte death (Matute, 2008), and hypoxia in neonates has been shown to lead to a reduction in myelination (Mottahedin et al., 2017).

The P2X7R is recognized as an important driver of inflammation (Di Virgilio et al., 2017). Because treating mouse pups with the anti-inflammatory drug minocycline attenuated the effects of P2X7R-OE, as well as the prominent expression of P2X7Rs in microglia and the anti-inflammatory tone in P2X7R-deficient mice after hypoxia, it is tempting to speculate that the effects of P2X7Rs on neonatal seizures are primarily mediated via inflammation. This would be in line with seizures in adults, where the seizure-suppressive effects of P2X7R are thought to be mediated, at least in part, via suppressing inflammatory pathways (Engel et al., 2021). Inflammatory messengers (e.g., cytokines) are well characterized in animal models and slice electrophysiology to modulate hyperexcitability by directly influencing ion channels and neurotransmitter release (Vezzani et al., 2019). In infant patients following NE, an elevation in circulating inflammatory molecules has been shown to correlate with a greater probability of developing epilepsy (Numis et al., 2019). Previous studies have demonstrated increased levels of microgliosis and cytokine release, particularly IL-1β, in this hypoxia-induced neonatal seizure model, with this being associated with neuronal damage and aberrant neuron morphology in the hippocampus in later life (Quinlan et al., 2019). Moreover, targeting inflammation during hypoxia has shown success in reducing neonatal seizure severity and to alleviate adverse long-term clinical outcomes (Quinlan et al., 2019; Wu et al., 2022).

Our results show that after hypoxia, there is an increase in the polarization of microglia to a pro-inflammatory state consistent to that of adult seizures, where an increased number of pro-inflammatory microglia were observed during epileptogenesis (Benson et al., 2015). Here, we show that when the expression of P2X7Rs is reduced, the microglial response is switched to an anti-inflammatory phenotype, thus potentially promoting tissue repair (Suenaga et al., 2015) and inhibiting of pro-inflammatory drive (Cherry et al., 2014). Of note, the depletion of microglia has been shown to worsen the seizure phenotype (Badimon et al., 2020), suggesting that targeting of specific inflammatory cascades (e.g., P2X7R-driven) may be of more benefit.

Through GO analysis, we observed a down-regulation of pathways involved in immunomodulation, such as the TGF-β signalling pathway, in line with P2X7R's known role in driving inflammatory processes (Di Virgilio et al., 2017). Other pathways include oxidative phosphorylation, among the main pathways dysregulated in *P2X7*$^{-/-}$

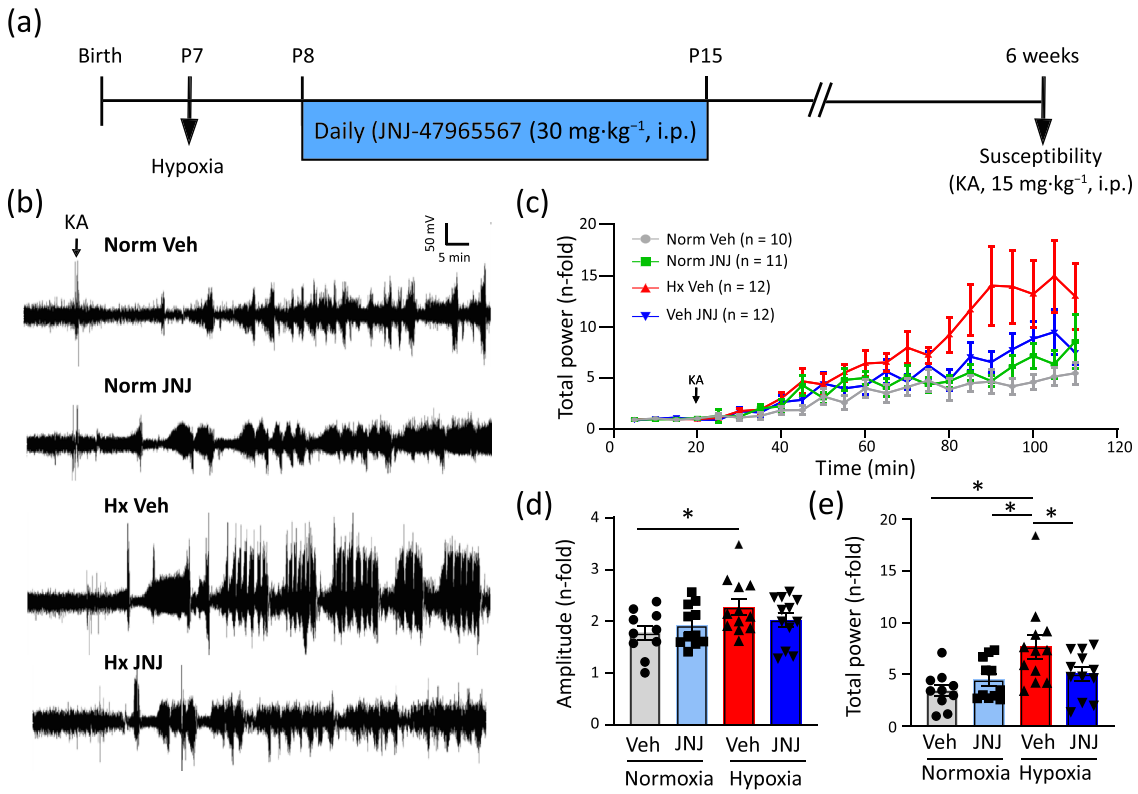

FIGURE 6 Antagonism of P2X7R after hypoxia reduces the susceptibility of mice to later-life seizures. (a) Schematic outlining the experimental paradigm, where mice were treated daily with 30 mg·kg^{-1} JNJ-47965567 for 7 days. At 6 weeks of age (i.e., 5 weeks post-hypoxic treatment), mice were injected with 15 mg·kg^{-1} KA to induce seizures and EEG was recorded. (b) Representative EEG traces from normoxic control vehicle-treated (Norm Veh), normoxic control JNJ-47965567-treated (Norm JNJ), hypoxic vehicle-treated (Hx Veh) and hypoxic JNJ-47965567-treated (Hx JNJ) mice after KA injection. EEG was recorded for 90 min after KA injection. (c) Graph showing EEG total power over time measured every 5 min for 90 min starting at the time of KA injection (one-way ANOVA with Fisher's post hoc test; n = 10 [Norm Veh], 11 [Norm JNJ], 12 [Hx Veh] and 12 [Hx JNJ]). Graphs showing (d) EEG amplitude and (e) EEG total power during a 90 min recording period starting at the time of KA treatment (one-way ANOVA with Fisher's post hoc test; n = 10 [Norm Veh], 11 [Norm JNJ], 12 [Hx Veh] and 12 [Hx JNJ]). *P < 0.05.

mice. The observed down-regulation in normoxic control *P2X7*$^{-/-}$ mouse pups aligns with a recent study, where P2X7R was found to be localized on the mitochondrial membrane where it was suggested to support mitochondrial energetics (Sarti et al., 2021). In contrast, under hypoxic conditions, genes implicated in oxidative phosphorylation were found to be up-regulated in *P2X7*$^{-/-}$ mouse pups, possibly indicative of an adaptive response of microglia to protect the brain. In support of this proposal, a recent study that sequenced isolated microglia after KA-induced status epilepticus (Bosco et al., 2018) observed that several genes encoding subunits of the complex 1 of the respiratory chain were up-regulated. Hence, microglia favouring oxidative respiration over glycolysis is representative of a less pro-inflammatory microglial phenotype (Orihuela et al., 2016). Moreover, the increase of oxidative phosphorylation observed may be indicative of microglia being in a less activated state due to perhaps a reduced initial seizure insult or via an increase of anti-inflammatory signalling. We also observed that *P2X7*$^{-/-}$ mice have a pronounced down-regulation of genes involved in glutamatergic signalling, both during normoxic conditions and after hypoxia. Of note, enhanced glutamatergic signalling is associated with epileptogenesis (Scimemi et al., 2006). Furthermore, **glutamate** efflux is increased in the perinatal brain following a hypoxic–ischaemic event (Silverstein et al., 1991), possibly contributing to neuronal damage following a hypoxic–ischaemic injury (Johnston, 2001). Therefore, a down-regulation of glutamatergic signalling may be one of the mechanisms by which P2X7R deficiency protects the brain from damage. P2X7R is well documented to modulate glutamatergic activity, where P2X7R facilitates glutamate release from astrocytes and neurons into the extracellular space, leading to excitotoxicity (Deuchars et al., 2001; Leon et al., 2008; Sperlagh et al., 2006).

Using treatments based on P2X7R antagonists, we demonstrate a disease-modifying effect of targeting P2X7R following hypoxia, with P2X7R antagonism able to prevent hypoxia-induced hyperexcitability. Of note, our treatment paradigm started 24 h after the initial insult, when acute symptomatic seizures as a result of hypoxia have mostly ceased. This result reinforces a previous study in which a disease-modifying effect was observed when the same P2X7R antagonist (JNJ-47965567) reduced seizures in an adult model of epilepsy (Jimenez-Pacheco et al., 2016). Current medications for neonatal seizures, including phenobarbital, are heavily associated with adverse

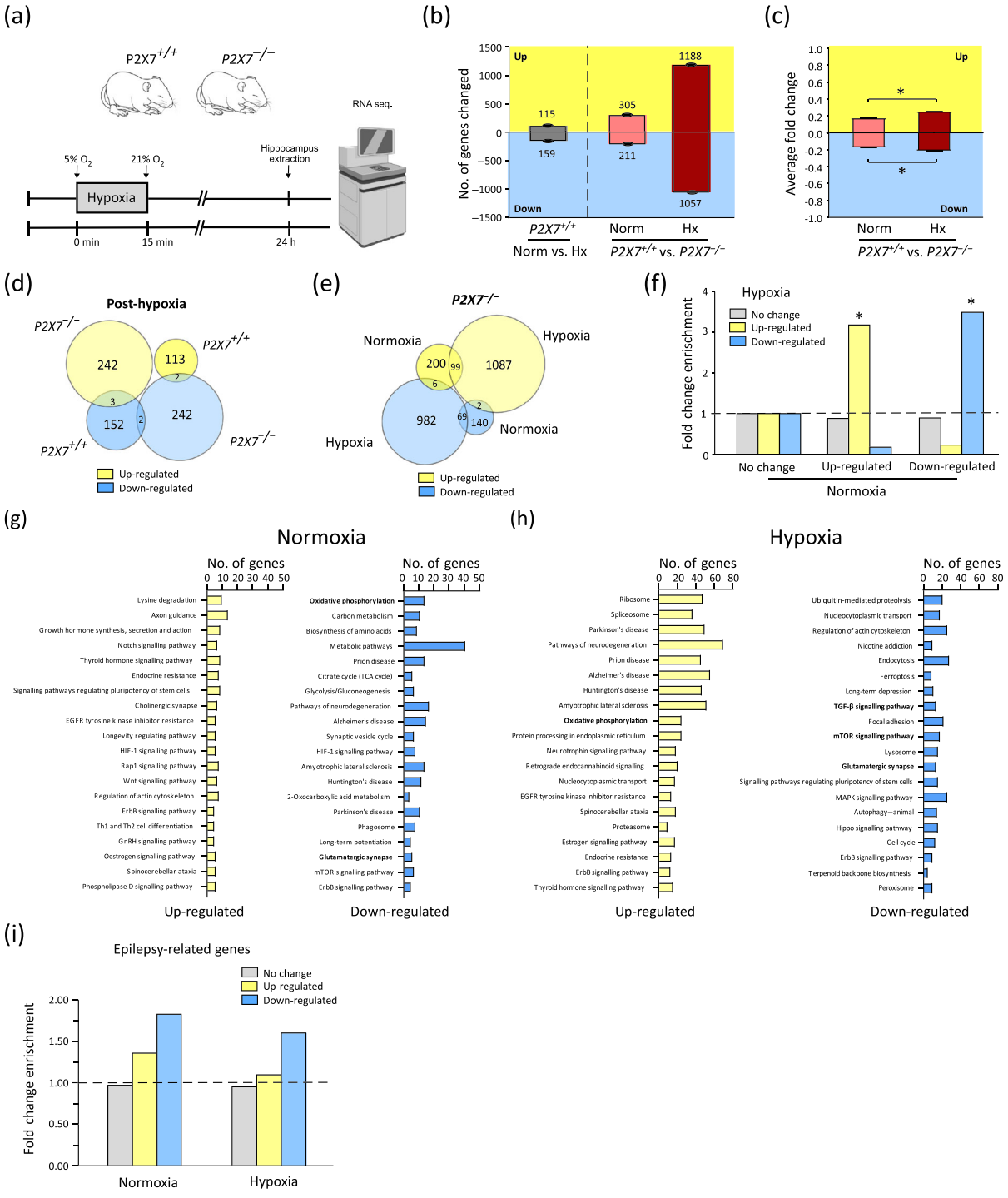

FIGURE 7 P2X7R-dependent gene changes in the hippocampus after hypoxia. (a) Schematic outlining the experimental paradigm. Hippocampi from *P2X7*$^{+/+}$ and *P2X7*$^{-/-}$ mice were taken 24 h following either normoxia or hypoxia and sent for RNA-sequencing analysis. (b) Number of gene changes in *P2X7*$^{+/+}$ mouse pups when comparing normoxic with hypoxic conditions (grey column), and gene changes when comparing *P2X7*$^{+/+}$ mice with *P2X7*$^{-/-}$ (n = 5 for all groups). (c) Average gene expression fold changes when comparing *P2X7*$^{+/+}$ mice with *P2X7*$^{-/-}$ during normoxic control conditions and 24 h after hypoxia (unpaired Student's *t* test; *P2X7*$^{+/+}$ vs. *P2X7*$^{-/-}$ [normoxia]: 305 [up-regulated] and 211 [down-regulated]; *P2X7*$^{+/+}$ vs. *P2X7*$^{-/-}$ [hypoxia]: 1188 [up-regulated] and 1057 [down-regulated]). (d) Venn diagram showing the number of up- and down-regulated genes unique and common to *P2X7*$^{+/+}$ and *P2X7*$^{-/-}$ mice after hypoxia. (e) Venn diagram showing the number of up- and down-regulated genes unique and common in *P2X7*$^{-/-}$ mice during both normoxic and post-hypoxic conditions. (f) Comparison of differentially expressed genes in normoxia versus hypoxia in *P2X7*$^{-/-}$ mice. The Y axis represents the FC enrichment between conditions. (g) Brain-specific pathways up-regulated and down-regulated between *P2X7*$^{+/+}$ and *P2X7*$^{-/-}$ mice under normoxic conditions. (h) Brain-specific pathways up- and down-regulated following hypoxic conditions. (i) Enrichment analysis of epilepsy-related genes in differentially expressed transcripts in both normoxic and hypoxic conditions in *P2X7*$^{-/-}$ mice. One-sided Fisher's exact test. *$P < 0.05$.

effects, including neurodegeneration and a greater predisposition to later-life seizures (Torolira et al., 2017), even when given alone in the absence of any pathology (Quinlan et al., 2018). We saw no evidence of adverse effects with JNJ-47965567, suggesting that this compound is safe to be targeted in the immature brain. However, a much more thorough safety profiling must be done in future studies.

Finally, we show that increased P2X7R expression reduces responsiveness to phenobarbital. This is in line with previous studies reporting that P2X7R-OE increases non-responsiveness to several ASMs during adult SE (Beamer et al., 2022). Therefore, the P2X7R may be one of the culprits in generating drug resistance during neonatal seizures, and hence, future studies should explore the therapeutic potential of P2X7R antagonists as adjunctive treatment for neonatal seizures.

One limitation of the present study is that we have used a mouse model of mild hypoxia. Future studies should investigate this in models with more severe pathology (e.g., models of HIE). Another limitation of our study is the strong focus on the hippocampus. Although previous research by us has shown that P2X7R expression was increased in the hippocampus after hypoxia, these increases also were observed in the cortex (Rodriguez-Alvarez et al., 2017). Moreover, global hypoxia-induced inflammatory processes are most likely activated throughout the brain; therefore, we could expect P2X7R expression and function to be increased in other brain structures, which may contribute to seizures and overall pathology in the model. Although outside of the scope of the present study, this should be addressed in the future. Because activation of the P2X7R requires relatively high levels of ATP that are normally only observed under pathological conditions (Surprenant et al., 1996), P2X7R-based treatments may lead to fewer side effects. Data have, however, also shown a role for P2X7Rs during physiological conditions including a role in neurogenesis (Leeson et al., 2019). This conclusion is reinforced through our sequencing analysis, where we found several pathways altered in mice lacking P2X7Rs under normal physiological conditions suggesting a role for P2X7Rs during normal development. Thus, future studies should carefully evaluate the safety profile of treatments based on P2X7R antagonism during development. Finally, the anticonvulsive and anti-epileptogenic effects observed when blocking the P2X7R suggest P2X7R activation during and after hypoxia. Future studies should determine when and where ATP is released during hypoxia, which will be critical to identify the optimal P2X7R-based treatment period.

5 | CONCLUSIONS

Our findings suggest that P2X7Rs act to potentiate hypoxia-induced neonatal seizures and that antagonism of P2X7Rs has an anticonvulsive action and can have long-term actions in reducing brain hyperexcitability, possibly via reducing pathological inflammation whilst promoting anti-inflammatory cascades.

AUTHOR CONTRIBUTIONS

Jonathon Smith: Conceptualization (equal); data curation (lead); formal analysis (equal); investigation (equal); methodology (equal); writing—original draft (equal); writing—review and editing (supporting). **Aida Menéndez Méndez:** Data curation (equal); formal analysis (equal); investigation (equal); methodology (equal); writing—review and editing (supporting). **Mariana Alves:** Data curation (supporting); formal analysis (supporting); investigation (supporting); writing—review and editing (supporting). **Alberto Parras:** Formal analysis (equal); investigation (equal); methodology (equal); writing—review and editing (supporting). **Giorgia Conte:** Formal analysis (supporting); writing—review and editing (supporting). **Anindya Bhattacharya:** Resources (equal); writing—review and editing (supporting). **Marc Ceusters:** Resources (equal); writing—review and editing (supporting). **Annette Nicke:** Resources (equal); writing—review and editing (supporting). **David C. Henshall:** Funding acquisition (equal); resources (equal); supervision (supporting); writing—review and editing (supporting). **Eva M. Jimenez-Mateos:** Conceptualization (equal); data curation (supporting); formal analysis (equal); investigation (equal); methodology (equal); supervision (supporting); writing—original draft (supporting); writing—review and editing (supporting). **Tobias Engel:** Conceptualization (lead); data curation (supporting); formal analysis (supporting); funding acquisition (lead); investigation (lead); methodology (supporting); project administration (lead); resources (lead); supervision (lead); writing—original draft (lead); writing—review and editing (lead).

ACKNOWLEDGEMENTS

This work was supported by funding from Science Foundation Ireland (17/CDA/4708, and co-funded under the European Regional Development Fund and by FutureNeuro industry partners 16/RC/3948), the European Union's Horizon 2020 research and innovation programme under the Marie Skłodowska-Curie grant agreement (No. 766124), the H2020 Marie Skłodowska-Curie Actions Individual Fellowship (No. 884956), the Deutsche Forschungsgemeinschaft (DFG, German Research Foundation, Project ID 335447717—SFB 1328, A15) and the Irish Research Council for Science, Engineering and Technology (Government of Ireland Postdoctoral Fellowship Programme, GOIPD/2020/865). Open access funding provided by IReL.

CONFLICT OF INTEREST STATEMENT

The authors declare no conflicts of interest. The funders had no role in the design of the study; in the collection, analyses or interpretation of data; in the writing of the manuscript; or in the decision to publish the results. The authors declare that this study received funding from FutureNeuro. The funder was not involved in the study design, collection, analysis, interpretation of data, the writing of this article or the decision to submit it for publication. Anindya Bhattacharya is, and Marc Ceusters was, an employee of Janssen Research and Development, but had no influence in the study design.

DECLARATION OF TRANSPARENCY AND SCIENTIFIC RIGOUR

This Declaration acknowledges that this paper adheres to the principles for transparent reporting and scientific rigour of preclinical research as stated in the *BJP* guidelines for Design & Analysis, Immunoblotting and Immunochemistry, and Animal Experimentation

and as recommended by funding agencies, publishers and other organizations engaged with supporting research.

DATA AVAILABILITY STATEMENT

The data that support the findings of this study are available from the corresponding author upon reasonable request.

REFERENCES

Alexander, S. P., Christopoulos, A., Davenport, A. P., Kelly, E., Mathie, A., Peters, J. A., Veale, E. L., Armstrong, J. F., Faccenda, E., Harding, S. D., Pawson, A. J., Southan, C., Davies, J. A., Abbracchio, M. P., Alexander, W., al-hosaini, K., Bäck, M., Barnes, N. M., Bathgate, R., … Ye, R. D. (2021). The Concise Guide to PHARMACOLOGY 2021/22: G protein-coupled receptors. *British Journal of Pharmacology*, *178*(Suppl 1), S27–S156. https://doi.org/10.1111/bph.15538

Alves, M., de Diego Garcia, L., Conte, G., Jimenez-Mateos, E. M., D'Orsi, B., Sanz-Rodriguez, A., Prehn, J. H. M., Henshall, D. C., & Engel, T. (2019). Context-specific switch from anti- to pro-epileptogenic function of the P2Y1 receptor in experimental epilepsy. *The Journal of Neuroscience*, *39*(27), 5377–5392. https://doi.org/10.1523/JNEUROSCI.0089-19.2019

Badimon, A., Strasburger, H. J., Ayata, P., Chen, X., Nair, A., Ikegami, A., Hwang, P., Chan, A. T., Graves, S. M., Uweru, J. O., Ledderose, C., Kutlu, M. G., Wheeler, M. A., Kahan, A., Ishikawa, M., Wang, Y. C., Loh, Y. H. E., Jiang, J. X., Surmeier, D. J., … Schaefer, A. (2020). Negative feedback control of neuronal activity by microglia. *Nature*, *586*(7829), 417–423. https://doi.org/10.1038/s41586-020-2777-8

Beamer, E., Fischer, W., & Engel, T. (2017). The ATP-gated P2X7 receptor as a target for the treatment of drug-resistant epilepsy. *Frontiers in Neuroscience*, *11*, 21. https://doi.org/10.3389/fnins.2017.00021

Beamer, E., Kuchukulla, M., Boison, D., & Engel, T. (2021). ATP and adenosine—Two players in the control of seizures and epilepsy development. *Progress in Neurobiology*, *204*, 102105. https://doi.org/10.1016/j.pneurobio.2021.102105

Beamer, E., Morgan, J., Alves, M., Menéndez Méndez, A., Morris, G., Zimmer, B., Conte, G., Diego-Garcia, L., Alarcón-Vila, C., Yiu Ng, N. K., Madden, S., Calzaferri, F., Ríos, C., García, A. G., Hamacher, M., Dinkel, K., Pelegrín, P., Henshall, D. C., Nicke, A., & Engel, T. (2022). Increased expression of the ATP-gated P2X7 receptor reduces responsiveness to anti-convulsants during status epilepticus in mice. *British Journal of Pharmacology*, *179*(12), 2986–3006. https://doi.org/10.1111/bph.15785

Benson, M. J., Manzanero, S., & Borges, K. (2015). Complex alterations in microglial M1/M2 markers during the development of epilepsy in two mouse models. *Epilepsia*, *56*(6), 895–905. https://doi.org/10.1111/epi.12960

Bosco, D. B., Zheng, J., Xu, Z., Peng, J., Eyo, U. B., Tang, K., Yan, C., Huang, J., Feng, L., Wu, G., Richardson, J. R., Wang, H., & Wu, L. J. (2018). RNAseq analysis of hippocampal microglia after kainic acid-induced seizures. *Molecular Brain*, *11*(1), 34. https://doi.org/10.1186/s13041-018-0376-5

Cherry, J. D., Olschowka, J. A., & O'Banion, M. K. (2014). Neuroinflammation and M2 microglia: The good, the bad, and the inflamed. *Journal of Neuroinflammation*, *11*, 98. https://doi.org/10.1186/1742-2094-11-98

Curtis, M. J., Alexander, S. P. H., Cirino, G., George, C. H., Kendall, D. A., Insel, P. A., Izzo, A. A., Ji, Y., Panettieri, R. A., Patel, H. H., Sobey, C. G., Stanford, S. C., Stanley, P., Stefanska, B., Stephens, G. J., Teixeira, M. M., Vergnolle, N., & Ahluwalia, A. (2022). Planning experiments: Updated guidance on experimental design and analysis and their reporting III. *British Journal of Pharmacology*, *179*, 3907–3913. https://doi.org/10.1111/bph.15868

Deuchars, S. A., Atkinson, L., Brooke, R. E., Musa, H., Milligan, C. J., Batten, T. F., Buckley, N. J., Parson, S. H., & Deuchars, J. (2001). Neuronal P2X7 receptors are targeted to presynaptic terminals in the central and peripheral nervous systems. *The Journal of Neuroscience*, *21*(18), 7143–7152. https://doi.org/10.1523/JNEUROSCI.21-18-07143.2001

Di Virgilio, F., Dal Ben, D., Sarti, A. C., Giuliani, A. L., & Falzoni, S. (2017). The P2X7 receptor in infection and inflammation. *Immunity*, *47*(1), 15–31. https://doi.org/10.1016/j.immuni.2017.06.020

Di Virgilio, F., Sarti, A. C., & Coutinho-Silva, R. (2020). Purinergic signaling, DAMPs, and inflammation. *American Journal of Physiology. Cell Physiology*, *318*(5), C832–C835. https://doi.org/10.1152/ajpcell.00053.2020

Engel, T., Gómez-Sintes, R., Alves, M., Jimenez-Mateos, E. M., Fernández-Nogales, M., Sanz-Rodriguez, A., Morgan, J., Beamer, E., Rodríguez-Matellán, A., Dunleavy, M., Sano, T., Avila, J., Medina, M., Hernandez, F., Lucas, J. J., & Henshall, D. C. (2018). Bi-directional genetic modulation of GSK-3β exacerbates hippocampal neuropathology in experimental status epilepticus. *Cell Death & Disease*, *9*(10), 969. https://doi.org/10.1038/s41419-018-0963-5

Engel, T., Gomez-Villafuertes, R., Tanaka, K., Mesuret, G., Sanz-Rodriguez, A., Garcia-Huerta, P., Miras-Portugal, M. T., Henshall, D. C., & Diaz-Hernandez, M. (2012). Seizure suppression and neuroprotection by targeting the purinergic P2X7 receptor during status epilepticus in mice. *The FASEB Journal*, *26*(4), 1616–1628. https://doi.org/10.1096/fj.11-196089

Engel, T., Smith, J., & Alves, M. (2021). Targeting neuroinflammation via purinergic P2 receptors for disease modification in drug-refractory epilepsy. *Journal of Inflammation Research*, *14*, 3367–3392. https://doi.org/10.2147/JIR.S287740

Epi4K Consortium, & Epilepsy Phenome/Genome Project. (2017). Ultra-rare genetic variation in common epilepsies: A case-control sequencing study. *Lancet Neurology*, *16*(2), 135–143. https://doi.org/10.1016/S1474-4422(16)30359-3

Feng, Y., Rhodes, P. G., & Bhatt, A. J. (2008). Neuroprotective effects of vascular endothelial growth factor following hypoxic ischemic brain injury in neonatal rats. *Pediatric Research*, *64*(4), 370–374. https://doi.org/10.1203/PDR.0b013e318180ebe6

Glass, H. C., Shellhaas, R. A., Wusthoff, C. J., Chang, T., Abend, N. S., Chu, C. J., Cilio, M. R., Glidden, D. V., Bonifacio, S. L., Massey, S., Tsuchida, T. N., Silverstein, F. S., Soul, J. S., Bergin, A. M., Dlugos, D., Ferriero, D. M., & Staley, K. (2016). Contemporary profile of seizures in neonates: A prospective cohort study. *The Journal of Pediatrics*, *174*, 98–103.e1. https://doi.org/10.1016/j.jpeds.2016.03.035

Hagberg, H., Mallard, C., Ferriero, D. M., Vannucci, S. J., Levison, S. W., Vexler, Z. S., & Gressens, P. (2015). The role of inflammation in perinatal brain injury. *Nature Reviews. Neurology*, *11*(4), 192–208. https://doi.org/10.1038/nrneurol.2015.13

Hellstrom-Westas, L., Boylan, G., & Agren, J. (2015). Systematic review of neonatal seizure management strategies provides guidance on antiepileptic treatment. *Acta Paediatrica*, *104*(2), 123–129. https://doi.org/10.1111/apa.12812

International League Against Epilepsy Consortium on Complex Epilepsies. (2018). Genome-wide mega-analysis identifies 16 loci and highlights diverse biological mechanisms in the common epilepsies. *Nature Communications*, *9*(1), 5269. https://doi.org/10.1038/s41467-018-07524-z

Jensen, F. E. (2009). Neonatal seizures: An update on mechanisms and management. *Clinics in Perinatology*, *36*(4), 881–900vii. https://doi.org/10.1016/j.clp.2009.08.001

Jimenez-Mateos, E. M., Engel, T., Merino-Serrais, P., McKiernan, R. C., Tanaka, K., Mouri, G., Sano, T., O'Tuathaigh, C., Waddington, J. L., Prenter, S., Delanty, N., Farrell, M. A., O'Brien, D. F., Conroy, R. M., Stallings, R. L., DeFelipe, J., & Henshall, D. C. (2012). Silencing microRNA-134 produces neuroprotective and prolonged seizure-suppressive effects. *Nature Medicine*, *18*(7), 1087–1094. https://doi.org/10.1038/nm.2834

Jimenez-Pacheco, A., Diaz-Hernandez, M., Arribas-Blázquez, M., Sanz-Rodriguez, A., Olivos-Oré, L. A., Artalejo, A. R., Alves, M., Letavic, M., Miras-Portugal, M. T., Conroy, R. M., Delanty, N., Farrell, M. A., O'Brien, D. F., Bhattacharya, A., Engel, T., & Henshall, D. C. (2016). Transient P2X7 receptor antagonism produces lasting reductions in spontaneous seizures and gliosis in experimental temporal lobe epilepsy. *The Journal of Neuroscience*, *36*(22), 5920–5932. https://doi.org/10.1523/JNEUROSCI.4009-15.2016

Johnston, M. V. (2001). Excitotoxicity in neonatal hypoxia. *Mental Retardation and Developmental Disabilities Research Reviews*, *7*(4), 229–234. https://doi.org/10.1002/mrdd.1032

Kaczmarek-Hajek, K., Zhang, J., Kopp, R., Grosche, A., Rissiek, B., Saul, A., Bruzzone, S., Engel, T., Jooss, T., Krautloher, A., Schuster, S., Magnus, T., Stadelmann, C., Sirko, S., Koch-Nolte, F., Eulenburg, V., & Nicke, A. (2018). Re-evaluation of neuronal P2X7 expression using novel mouse models and a P2X7-specific nanobody. *eLife*, *7*, e36217. https://doi.org/10.7554/eLife.36217

Leavy, A., & Jimenez Mateos, E. M. (2020). Perinatal brain injury and inflammation: Lessons from experimental murine models. *Cell*, *9*(12), 2640. https://doi.org/10.3390/cells9122640

Leeson, H. C., Chan-Ling, T., Lovelace, M. D., Brownlie, J. C., Gu, B. J., & Weible, M. W. (2019). P2X7 receptor signaling during adult hippocampal neurogenesis. *Neural Regeneration Research*, *14*(10), 1684–1694. https://doi.org/10.4103/1673-5374.257510

Leon, D., Sanchez-Nogueiro, J., Marin-Garcia, P., & Miras-Portugal, M. A. (2008). Glutamate release and synapsin-I phosphorylation induced by P2X7 receptors activation in cerebellar granule neurons. *Neurochemistry International*, *52*(6), 1148–1159. https://doi.org/10.1016/j.neuint.2007.12.004

Lilley, E., Stanford, S. C., Kendall, D. E., Alexander, S. P. H., Cirino, G., Docherty, J. R., George, C. H., Insel, P. A., Izzo, A. A., Ji, Y., Panettieri, R. A., Sobey, C. G., Stefanska, B., Stephens, G., Teixeira, M., & Ahluwalia, A. (2020). ARRIVE 2.0 and the British Journal of Pharmacology: Updated guidance for 2020. *British Journal of Pharmacology*, *177*(16), 3611–3616. https://doi.org/10.1111/bph.15178

Matute, C. (2008). P2X7 receptors in oligodendrocytes: A novel target for neuroprotection. *Molecular Neurobiology*, *38*(2), 123–128. https://doi.org/10.1007/s12035-008-8028-x

Monif, M., Reid, C. A., Powell, K. L., Smart, M. L., & Williams, D. A. (2009). The P2X7 receptor drives microglial activation and proliferation: A trophic role for P2X7R pore. *The Journal of Neuroscience*, *29*(12), 3781–3791. https://doi.org/10.1523/JNEUROSCI.5512-08.2009

Morgan, J., Alves, M., Conte, G., Menéndez-Méndez, A., de Diego-Garcia, L., de Leo, G., Beamer, E., Smith, J., Nicke, A., & Engel, T. (2020). Characterization of the expression of the ATP-gated P2X7 receptor following status epilepticus and during epilepsy using a P2X7-EGFP reporter mouse. *Neuroscience Bulletin*, *36*(11), 1242–1258. https://doi.org/10.1007/s12264-020-00573-9

Mottahedin, A., Svedin, P., Nair, S., Mohn, C. J., Wang, X., Hagberg, H., Ek, J., & Mallard, C. (2017). Systemic activation of toll-like receptor 2 suppresses mitochondrial respiration and exacerbates hypoxic–ischemic injury in the developing brain. *Journal of Cerebral Blood Flow and Metabolism*, *37*(4), 1192–1198. https://doi.org/10.1177/0271678X17691292

Numis, A. L., Foster-Barber, A., Deng, X., Rogers, E. E., Barkovich, A. J., Ferriero, D. M., & Glass, H. C. (2019). Early changes in pro-inflammatory cytokine levels in neonates with encephalopathy are associated with remote epilepsy. *Pediatric Research*, *86*(5), 616–621. https://doi.org/10.1038/s41390-019-0473-x

Orihuela, R., McPherson, C. A., & Harry, G. J. (2016). Microglial M1/M2 polarization and metabolic states. *British Journal of Pharmacology*, *173*(4), 649–665. https://doi.org/10.1111/bph.13139

Parras, A., de Diego-Garcia, L., Alves, M., Beamer, E., Conte, G., Jimenez-Mateos, E. M., Morgan, J., Ollà, I., Hernandez-Santana, Y., Delanty, N., Farrell, M. A., O'Brien, D. F., Ocampo, A., Henshall, D. C., Méndez, R., Lucas, J. J., & Engel, T. (2020). Polyadenylation of mRNA as a novel regulatory mechanism of gene expression in temporal lobe epilepsy. *Brain*, *143*, 2139–2153. https://doi.org/10.1093/brain/awaa168

Percie du Sert, N., Hurst, V., Ahluwalia, A., Alam, S., Avey, M. T., Baker, M., Browne, W. J., Clark, A., Cuthill, I. C., Dirnagl, U., Emerson, M., Garner, P., Holgate, S. T., Howells, D. W., Karp, N. A., Lazic, S. E., Lidster, K., MacCallum, C. J., Macleod, M., … Würbel, H. (2020). The ARRIVE guidelines 2.0: Updated guidelines for reporting animal research. *PLoS Biology*, *18*(7), e3000410. https://doi.org/10.1371/journal.pbio.3000410

Pressler, R. M., Cilio, M. R., Mizrahi, E. M., Moshé, S. L., Nunes, M. L., Plouin, P., Vanhatalo, S., Yozawitz, E., de Vries, L. S., Puthenveettil Vinayan, K., Triki, C. C., Wilmshurst, J. M., Yamamoto, H., & Zuberi, S. M. (2021). The ILAE classification of seizures and the epilepsies: Modification for seizures in the neonate. Position paper by the ILAE Task Force on Neonatal Seizures. *Epilepsia*, *62*(3), 615–628. https://doi.org/10.1111/epi.16815

Quinlan, S., Merino-Serrais, P., di Grande, A., Dussmann, H., Prehn, J. H. M., Ní Chonghaile, T., Henshall, D. C., & Jimenez-Mateos, E. M. (2019). The anti-inflammatory compound candesartan cilexetil improves neurological outcomes in a mouse model of neonatal hypoxia. *Frontiers in Immunology*, *10*, 1752. https://doi.org/10.3389/fimmu.2019.01752

Quinlan, S. M. M., Rodriguez-Alvarez, N., Molloy, E. J., Madden, S. F., Boylan, G. B., Henshall, D. C., & Jimenez-Mateos, E. M. (2018). Complex spectrum of phenobarbital effects in a mouse model of neonatal hypoxia-induced seizures. *Scientific Reports*, *8*(1), 9986. https://doi.org/10.1038/s41598-018-28044-2

Ramantani, G., Schmitt, B., Plecko, B., Pressler, R. M., Wohlrab, G., Klebermass-Schrehof, K., Hagmann, C., Pisani, F., & Boylan, G. B. (2019). Neonatal seizures—Are we there yet? *Neuropediatrics*, *50*(5), 280–293. https://doi.org/10.1055/s-0039-1693149

Rodriguez-Alvarez, N., Jimenez-Mateos, E. M., Dunleavy, M., Waddington, J. L., Boylan, G. B., & Henshall, D. C. (2015). Effects of hypoxia-induced neonatal seizures on acute hippocampal injury and later-life seizure susceptibility and anxiety-related behavior in mice. *Neurobiology of Disease*, *83*, 100–114. https://doi.org/10.1016/j.nbd.2015.08.023

Rodriguez-Alvarez, N., Jimenez-Mateos, E. M., Engel, T., Quinlan, S., Reschke, C. R., Conroy, R. M., Bhattacharya, A., Boylan, G. B., & Henshall, D. C. (2017). Effects of P2X7 receptor antagonists on hypoxia-induced neonatal seizures in mice. *Neuropharmacology*, *116*, 351–363. https://doi.org/10.1016/j.neuropharm.2017.01.005

Sarti, A. C., Vultaggio-Poma, V., Falzoni, S., Missiroli, S., Giuliani, A. L., Boldrini, P., Bonora, M., Faita, F., di Lascio, N., Kusmic, C., Solini, A., Novello, S., Morari, M., Rossato, M., Wieckowski, M. R., Giorgi, C., Pinton, P., & di Virgilio, F. (2021). Mitochondrial P2X7 receptor localization modulates energy metabolism enhancing physical performance. *Function (Oxford, England)*, *2*(2), zqab005. https://doi.org/10.1093/function/zqab005

Scimemi, A., Schorge, S., Kullmann, D. M., & Walker, M. C. (2006). Epileptogenesis is associated with enhanced glutamatergic transmission in the perforant path. *Journal of Neurophysiology*, *95*(2), 1213–1220. https://doi.org/10.1152/jn.00680.2005

Semple, B. D., Blomgren, K., Gimlin, K., Ferriero, D. M., & Noble-Haeusslein, L. J. (2013). Brain development in rodents and humans: Identifying benchmarks of maturation and vulnerability to injury across species. *Progress in Neurobiology*, *106-107*, 1–16. https://doi.org/10.1016/j.pneurobio.2013.04.001

Silverstein, F. S., Naik, B., & Simpson, J. (1991). Hypoxia-ischemia stimulates hippocampal glutamate efflux in perinatal rat brain: An in vivo microdialysis study. *Pediatric Research*, *30*(6), 587–590. https://doi.org/10.1203/00006450-199112000-00021

Sperlagh, B., Vizi, E. S., Wirkner, K., & Illes, P. (2006). P2X7 receptors in the nervous system. *Progress in Neurobiology*, *78*(6), 327–346. https://doi.org/10.1016/j.pneurobio.2006.03.007

Suenaga, J., Hu, X., Pu, H., Shi, Y., Hassan, S. H., Xu, M., Leak, R. K., Stetler, R. A., Gao, Y., & Chen, J. (2015). White matter injury and microglia/macrophage polarization are strongly linked with age-related long-term deficits in neurological function after stroke. *Experimental Neurology*, *272*, 109–119. https://doi.org/10.1016/j.expneurol.2015.03.021

Surprenant, A., Rassendren, F., Kawashima, E., North, R. A., & Buell, G. (1996). The cytolytic P_{2Z} receptor for extracellular ATP identified as a P_{2X} receptor ($P2X_7$). *Science*, *272*(5262), 735–738. https://doi.org/10.1126/science.272.5262.735

Torolira, D., Suchomelova, L., Wasterlain, C. G., & Niquet, J. (2017). Phenobarbital and midazolam increase neonatal seizure-associated neuronal injury. *Annals of Neurology*, *82*(1), 115–120. https://doi.org/10.1002/ana.24967

Vezzani, A., Balosso, S., & Ravizza, T. (2019). Neuroinflammatory pathways as treatment targets and biomarkers in epilepsy. *Nature Reviews. Neurology*, *15*(8), 459–472. https://doi.org/10.1038/s41582-019-0217-x

Wagner, C. B., Kreimer, A. M., Carrillo, N. P., Autry, E., Schadler, A., Cook, A. M., & Leung, N. R. (2021). Levetiracetam compared to phenobarbital as a first line therapy for neonatal seizures: An unexpected influence of benzodiazepines on seizure response. *Journal of Pediatric Pharmacology and Therapeutics*, *26*(2), 144–150. https://doi.org/10.5863/1551-6776-26.2.144

Wang, J., Lin, Z. J., Liu, L., Xu, H. Q., Shi, Y. W., Yi, Y. H., He, N., & Liao, W. P. (2017). Epilepsy-associated genes. *Seizure*, *44*, 11–20. https://doi.org/10.1016/j.seizure.2016.11.030

Wu, Y., Wei, H., Li, P., Zhao, H., Li, R., & Yang, F. (2022). Quercetin administration following hypoxia-induced neonatal brain damage attenuates later-life seizure susceptibility and anxiety-related behavior: Modulating inflammatory response. *Frontiers in Pediatrics*, *10*, 791815. https://doi.org/10.3389/fped.2022.791815

SUPPORTING INFORMATION

Additional supporting information can be found online in the Supporting Information section at the end of this article.

How to cite this article: Smith, J., Menéndez Méndez, A., Alves, M., Parras, A., Conte, G., Bhattacharya, A., Ceusters, M., Nicke, A., Henshall, D. C., Jimenez-Mateos, E. M., & Engel, T. (2023). The P2X7 receptor contributes to seizures and inflammation-driven long-lasting brain hyperexcitability following hypoxia in neonatal mice. *British Journal of Pharmacology*, *180*(13), 1710–1729. https://doi.org/10.1111/bph.16033